USGS
science for a changing world

Groundwater Ages from the Freshwater Zone of the Edwards Aquifer, Uvalde County, Texas—Insights into Groundwater Flow and Recharge

Scientific Investigations Report 2015–5163

U.S. Department of the Interior
U.S. Geological Survey

Groundwater Ages from the Freshwater Zone of the Edwards Aquifer, Uvalde County, Texas—Insights into Groundwater Flow and Recharge

By Andrew G. Hunt, Gary P. Landis, and Jason R. Faith

Scientific Investigations Report 2015–5163

U.S. Department of the Interior
U.S. Geological Survey

U.S. Department of the Interior
SALLY JEWELL, Secretary

U.S. Geological Survey
Suzette M. Kimball, Director

U.S. Geological Survey, Reston, Virginia: 2016

For more information on the USGS—the Federal source for science about the Earth, its natural and living resources, natural hazards, and the environment—visit http://www.usgs.gov or call 1–888–ASK–USGS.

For an overview of USGS information products, including maps, imagery, and publications, visit http://www.usgs.gov/pubprod/.

Suggested citation:
Hunt, A.G., Landis, G.P., and Faith, J.R., 2016, Groundwater ages from the freshwater zone of the Edwards Aquifer, Uvalde County, Texas—Insights into groundwater flow and recharge: U.S. Geological Survey Scientific Investigations Report 2015–5163, 28 p., http://dx.doi.org/10.3133/sir20155163.

ISSN 2328-0328 (online)

Acknowledgments

Primary funding for this project was provided by the Edwards Aquifer Authority (EAA), and U.S. Geological Survey Mendenhall Program. The authors would like to thank Edwards Aquifer Authority and San Antonio Water System's field personnel for their help in sampling, and we would also thank the municipalities of Sabinal, Knippa, and Uvalde for access to production wells.

Contents

Figures

Tables

Conversion Factors

Inch/Pound to SI

Multiply	By	To obtain
	Length	
inch (in.)	2.54	centimeter (cm)
inch (in.)	25.4	millimeter (mm)
	Volume	
ounce, fluid (fl. oz)	0.02957	liter (L)
pint (pt)	0.4732	liter (L)
quart (qt)	0.9464	liter (L)
gallon (gal)	3.785	liter (L)
	Flow rate	
gallon per minute (gal/min)	0.06309	liter per second (L/s)
	Mass	
ounce, avoirdupois (oz)	28.35	gram (g)
pound, avoirdupois (lb)	0.4536	kilogram (kg)
	Pressure	
atmosphere, standard (atm)	101.3	kilopascal (kPa)
bar	100	kilopascal (kPa)
inch of mercury at 60 ºF (in Hg)	3.377	kilopascal (kPa)

SI to Inch/Pound

Multiply	By	To obtain
	Length	
centimeter (cm)	0.3937	inch (in.)
millimeter (mm)	0.03937	inch (in.)
	Volume	
liter (L)	33.82	ounce, fluid (fl. oz)
liter (L)	2.113	pint (pt)
liter (L)	1.057	quart (qt)
liter (L)	0.2642	gallon (gal)
cubic centimeter (cm^3)	0.06102	cubic inch (in^3)
liter (L)	61.02	cubic inch (in^3)
	Flow rate	
liter per second (L/s)	15.85	gallon per minute (gal/min)
	Mass	
gram (g)	0.03527	ounce, avoirdupois (oz)
kilogram (kg)	2.205	pound avoirdupois (lb)
	Pressure	
kilopascal (kPa)	0.009869	atmosphere, standard (atm)
kilopascal (kPa)	0.01	bar
kilopascal (kPa)	0.2961	inch of mercury at 60 °F (in Hg)

Temperature in degrees Celsius (°C) may be converted to degrees Fahrenheit (°F) as follows:
°F = (1.8×°C)+32

Temperature in degrees Fahrenheit (°F) may be converted to degrees Celsius (°C) as follows:
°C = (°F–32)/1.8

Temperature in degrees Celsius (°C) may be converted to degrees Kelvin (°K) as follows:
°K =°C–273.15

Temperature in degrees Kelvin (°K) may be converted to degrees Celsius (°C) as follows:
°C =°K+273.15

Molar volume is defined at 1 atmosphere pressure and 0 °C as: 1 mole = 22.414 liters.

Abbreviations

AEW	air equilibrated water
Ar	argon
^{36}Ar	argon-36
^{38}Ar	argon-38
^{40}Ar	argon-40
cm^3	cubic centimeter
cm^3/cm^3	cubic centimeter per cubic centimeter
cm^3STP	cubic centimeter at standard temperature and pressure
cm^3STP/g_{H2O}	cubic centimeter at standard temperature and pressure per gram of water
CFC	chlorofluorocarbons
CH_4	methane
H_2	hydrogen
^3H	tritium
He	helium
^3He	helium-3
^4He	helium-4
Kr	krypton
^{84}Kr	krypton-84
^{86}Kr	krypton-86
mL	milliliter

N_2	nitrogen
Ne	neon
^{20}Ne	neon-20
^{21}Ne	neon-21
^{22}Ne	neon-22
NGRT	noble gas recharge temperature
O_2	oxygen
*P*atm	atmospheric pressure
STP	standard temperature and pressure (0 °C, 1 atmosphere)
Xe	xenon
^{130}Xe	xenon-130
^{132}Xe	xenon-132
USGS NGL	U.S. Geological Survey Noble Gas Laboratory

Symbols

>	greater than
<	less than
>>	much greater than
⇔	equivalent
≈	approximately (nearly) equal to
°	degree
°C	degrees Celsius
°K	degrees Kelvin
%	percent
±	plus or minus

Groundwater Ages from the Freshwater Zone of the Edwards Aquifer, Uvalde County, Texas—Insights into Groundwater Flow and Recharge

By Andrew G. Hunt, Gary P. Landis, and Jason R. Faith

Abstract

Tritium–helium-3 groundwater ages of the Edwards aquifer in south-central Texas were determined as part of a long-term study of groundwater flow and recharge in the Edwards and Trinity aquifers. These ages help to define groundwater residence times and to provide constraints for calibration of groundwater flow models. A suite of 17 samples from public and private supply wells within Uvalde County were collected for active and noble gases, and for tritium–helium-3 analyses from the confined and unconfined parts of the Edwards aquifer. Samples were collected from monitoring wells at discrete depths in open boreholes as well as from integrated pumped well-head samples. The data indicate a fairly uniform groundwater flow system within an otherwise structurally complex geologic environment comprised of regionally and locally faulted rock units, igneous intrusions, and karst features within carbonate rocks. Apparent ages show moderate, downward average, linear velocities in the Uvalde area with increasing age to the east along a regional groundwater flow path. Though the apparent age data show a fairly consistent distribution across the study area, many apparent ages indicate mixing of both modern (less than 60 years) and premodern (greater than 60 years) waters. This mixing is most evident along the "bad water" line, an arbitrary delineation of 1,000 milligrams per liter dissolved solids that separates the freshwater zone of the Edwards aquifer from the downdip saline water zone. Mixing of modern and premodern waters also is indicated within the unconfined zone of the aquifer by high excess helium concentrations in young waters. Excess helium anomalies in the unconfined aquifer are consistent with possible subsurface discharge of premodern groundwater from the underlying Trinity aquifer into the younger groundwater of the Edwards aquifer.

Introduction

The Edwards aquifer is one of the most permeable and productive aquifers in the world. The aquifer is a primary water source for an ever expanding population in south-central Texas (fig. 1*A*). Demand for water in this semiarid region of Texas includes municipal, agricultural, military, domestic, and recreational water use; Federal mandates also exist to protect listed endangered species that dwell in the spring discharges emanating from the aquifer. Geologic, geochemical, and geophysical studies combined with hydrologic models aid water-resource managers in developing long- and short-range strategies for optimal groundwater use and resource management that will balance increasing demands on the aquifer system. The aquifer consists of fractured limestone in the Balcones fault zone and associated karst features with fracture- and conduit-flow control of groundwater, a prominent downdip saline zone, and the presence of igneous hypabyssal alkalic stock intrusions.

Groundwater ages can provide a useful tool to aid traditional methods used for aquifer characterization. Traditional methods such as measurement of water levels, analysis of basic groundwater chemistry, and field or laboratory hydraulic conductivity tests can be used to assess horizontal and vertical hydraulic gradients, fluid flow directions, and to derive average linear velocities along flow vectors. Results of groundwater dating techniques and geophysical well-log analysis aid in the conceptual and computational modeling of groundwater flow. The results analyzed in this report are for the western part of the Edwards aquifer within Uvalde County, Texas (fig. 1*B*).

Overview of Groundwater Age

Groundwater age data commonly are misinterpreted when reporting groundwater flow studies; therefore, the data require an operational definition and definition of significance of age. The groundwater age is not the actual age of the water, but represents the mean residence time of a parcel of groundwater in an aquifer after isolation from the atmosphere. For an aquifer, mean residence time for the groundwater has implications for potential sustainability of the resource, understanding recharge, contaminant transport, and effects on groundwater quality. Young-age groundwaters typically imply high flow rates sustained by rapid recharge into the aquifer, and are an indicator that the resource is likely to be sustainable. Such groundwaters are also vulnerable to anthropogenic pollutants and other adverse effects to water quality. In contrast,

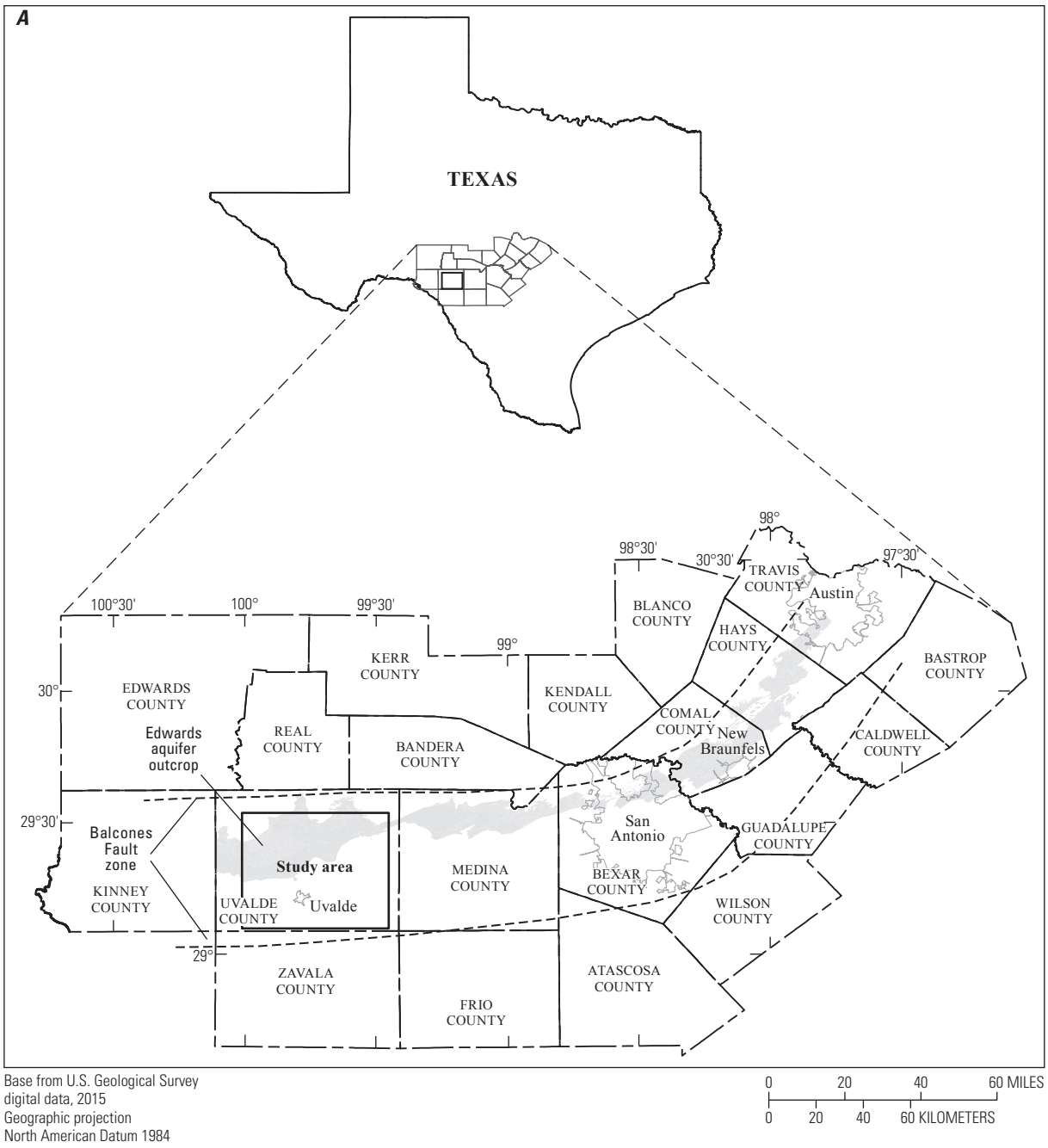

Figure 1. *A*, Location of study area with inset of Uvalde County, Texas. *B*, Sample locations, major faults with relative offsets, and approximate location of the Uvalde Salient. The freshwater/saline water transition is indicated as concentration equipotentials for 1,000 and 3,000 milligrams per liter (mg/L) of total dissolved solids after Shultz (1994). See table 1 for sample location symbols.

extremely old groundwaters may be less vulnerable to anthropogenic contaminants, but unable to sustain use because of the long mean residence time between recharge and extraction. Such resources become depleted with time from use and lack of sustaining recharge.

A useful interpretation of groundwater age is to classify waters with respect to connection to present-day hydrologic cycling. If "modern" groundwaters are those recharged within the past few decades and are part of the active hydrologic cycle (Clark and Fritz, 1999), then an indicator of "modern" groundwater is the presence of tritium (^{3}H). Tritium is the radioactive isotope of hydrogen, mainly derived from atmospheric thermonuclear device testing from 1951 to 1976, and from a small natural background level of cosmogenic tritium produced in the upper atmosphere. The ^{3}H atom is incorporated into the atmospheric water molecule and introduced into recharging groundwaters with precipitation. Given the thermonuclear and cosmogenic production rates and a

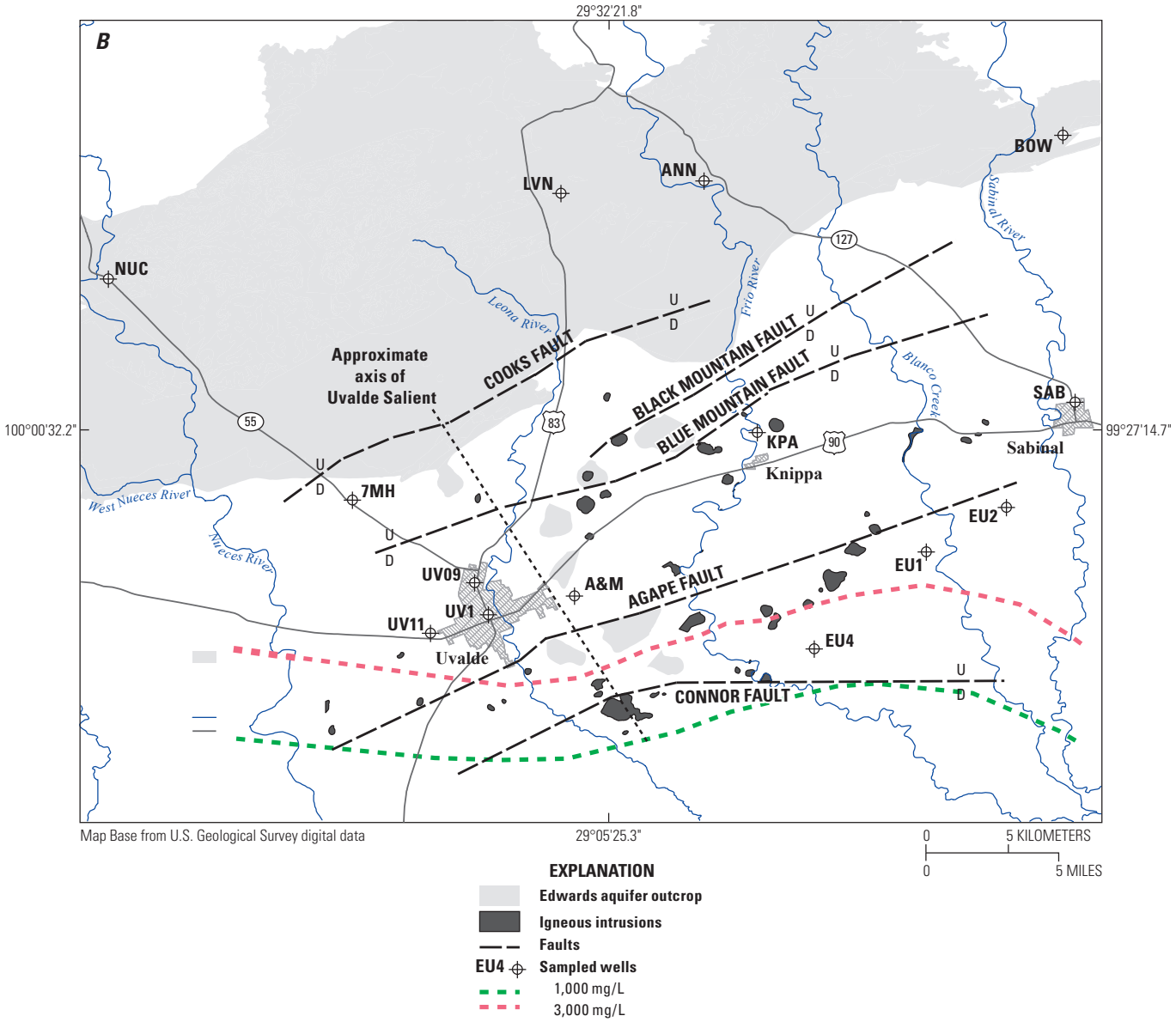

Figure 1. *A*, Location of study area with inset of Uvalde County, Texas. *B*, Sample locations, major faults with relative offsets, and approximate location of the Uvalde Salient. The freshwater/saline water transition is indicated as concentration equipotentials for 1,000 and 3,000 milligrams per liter (mg/L) of total dissolved solids after Shultz (1994). See table 1 for sample location symbols.—Continued

known 12.32 year half-life (Lucas and Unterweger, 2000), and recharge efficiency, concentrations of ^{3}H diminish to below detectable limits after approximately 4 to 5 half-lives or 49.3 to 61.7 years. As a convention, waters containing ^{3}H are modern groundwaters (less than 60 years of apparent age) and waters devoid of ^{3}H are submodern or premodern (greater than 60 years of apparent age).

Techniques for the accurate measurement of groundwater age are varied. In general, the technique should address exactly what is being dated, how it is introduced into the groundwater flow system, when the "clock" is started for the technique, what affects the interpretation of the analytical components involved, and whether there are any interferences in the subsurface that affect the calculation of age. The basis of many of these techniques relies on knowing the rates of introduction of elements or chemical species to the groundwater and equating the apparent age by matching concentrations to known input concentrations (for example, chlorofluorocarbons (CFCs) and sulfur hexafluoride), or known input of a short- or long-lived radioisotope to the groundwater and then determining age based on measured activity and known decay rate (that is, ^{3}H, ^{14}C, ^{39}Ar, ^{81}Kr). The conservative chemical nature of environmental tracers used for age dating (nonreactive, neither consumed nor produced by chemical reactions) allows for best estimates of an absolute age. However, integration of several sources of recharge with different ages through hydrodynamic mixing along convergent flow paths yields a composite and ambiguous groundwater age (Clark and Fritz, 1999), and the

effect of a mixing process on the calculated age differs with each tracer. For these reasons, the age determined by any specific technique is an apparent age. An extreme example of this would be when a known amount of modern recharge water containing a fixed concentration of CFCs and ^{3}H mixes with premodern water, resulting in a dilution of the environmental tracers. The calculated age resulting from dilution causes the ^{3}H apparent age to be younger than the actual age of the modern water while the apparent age derived from the CFCs is older. This discrepancy in apparent ages is because the ^{3}H age is derived from an input curve that decreases through time while the CFC age is from an input curve that increased with time until the late 1990s. An apparent age attributed to groundwater is useful when the technique and conditions of determination are understood. Age discrepancies between different techniques are a result of incomplete accounting of hydrogeologic-geochemical processes affecting the sample.

^{3}H-^{3}He Age

The ^{3}H-^{3}He method of dating modern groundwaters (Schlosser, 1992; Solomon and Cook, 2000) exploits the radioactive "parent-daughter" decay. The ^{3}H-^{3}He method results from the introduction of naturally occurring ^{3}H (as part of the tritiated water molecule) to the aquifer during recharge. As the groundwater moves away from the water table with continued recharge, the ^{3}H contained in the water molecule decays to ^{3}He, a dissolved gas. The "clock" starts after isolation from the atmosphere (about 1 meter [m] below the water table because of possible back diffusion of ^{3}He) and the age obtained in this case represents the time from isolation from the atmosphere. The transport of both the ^{3}H in the form of water and ^{3}He as a dissolved gas in the groundwater is considered highly conservative, and because the age calculation is based on both the parent and daughter isotopes and known rate of decay, the method is fairly insensitive to mixing. In the case of mixing with a premodern end member (void in both parent and daughter isotopes), the daughter to parent ratio is preserved as the apparent age of the modern groundwater component. For the binary mixing of two modern waters, the calculated apparent age actually represents an average age of the two end-member components.

The ^{3}H-^{3}He method relies on the measurement of not only the ^{3}H contained in the groundwater, but also the amount of tritiogenically derived ^{3}He (^{3}He*). Helium in the atmosphere has a homogeneous composition that is made up of two isotopes (^{3}He and ^{4}He) with a concentration of 5.24 parts per million (ppm) and isotopic ratio of 1.384×10^{-6} for ^{3}He/^{4}He. As recharged groundwater enters an aquifer, the concentration of helium in the groundwater is in equilibrium with the atmosphere (air saturated water [ASW]) at the temperature of recharge. This water may also have extra helium from excess atmospheric gas trapped during recharge (excess air), which is forced into solution with increasing hydrostatic pressure as isolated bubbles are entrained deeper into the zone of recharge. In order to resolve the tritiogenic ^{3}He from the total ^{3}He in a sample of groundwater, the initial concentration of ^{3}He associated with recharge and excess gas is computed by measuring other dissolved atmospheric gases contained within the sample. Neon, argon, krypton, and xenon are measured, along with total helium and the helium isotopic ratio. The temperature and pressure of groundwater recharge is computed using known physiochemical solubility parameters for atmospheric gas, as well as parameters for excess air compositions. These calculated conditions define the amount of excess ^{3}He (Stute and Sonntag, 1992, Aeschbach-Hertig, Peeters, and others, 1999; Ballentine and Hall, 1999). The remaining excess ^{3}He is a combination of the tritium-derived ^{3}He and a terrigenic ^{3}He produced from thermal neutron fluxes derived from decay of radioactive nuclides within the crust, and from a flux of primordial helium released from the Earth's interior. In most modern waters the terrigenic helium component is not present, but in older waters terrigenic helium can dominate the ^{3}He composition. Using similar methods to those used for resolving the dissolved atmospheric gas components, excess helium is calculated. Using a characteristic isotopic ratio for the excess helium component, terrigenic ^{3}He can be defined, and thus the remaining amount of ^{3}He from the total ^{3}He measured is derived from tritium. This process of ^{3}He resolution for the groundwater dating method gives insight into recharge conditions and possible subsurface conditions that can affect the dissolved gas composition.

Uvalde County

The study area is located approximately 100 kilometers west of San Antonio, Texas in Uvalde County (fig. 1*A*). The area is largely scattered agricultural lands and the municipalities of Uvalde, Knippa, and Sabinal, with an estimated population of approximately 26,000 (U.S. Census Bureau, 2008), most of which reside in Uvalde. The region is characterized as a semiarid climate and receives an average rainfall of approximately 60 centimeters per year with a mean annual temperature of 20 °C (National Oceanic and Atmospheric Administration, 2006). Carbonate bedrock units of the Edwards aquifer crop out in the northern part of the county and dip gently to the south, becoming a confined flow system in the southern part of the county (fig. 1*B*). The area lies in the Balcones fault zone, a series of east-west normal faults that are downthrown to the south. The bedrock units of interest in the area range from Lower Cretaceous units of the lower confining unit and the Edwards aquifer to Upper Cretaceous to Tertiary units of the upper confining units. For purposes of this report the downdip limit of unmixed, freshwater infiltration in the Edwards aquifer is defined by the 1,000 mg/L of total dissolved solids as recognized by Schulz (1994). This arbitrary demarcation is shown in Figure 1*B* as equipotential lines of TDS (total dissolved solids) concentration. South of this demarcation the groundwaters contained in the Edwards

aquifer are characterized by mixed saline formation waters that do not appear to be well connected to the hydraulically active, updip freshwater zone.

Hydrogeologic Setting

Geologic Setting

The carbonate-rich formations comprising the Edwards aquifer in Uvalde County consist of two depositional facies associated with early Cretaceous marine transgressive/regressive sediment cycles that were deposited over the Glen Rose Limestone (early Cretaceous), a sequence of thinly bedded limestone and marl that comprise the confining unit below the aquifer (Clark and Small, 1997; Clark, 2003). In the western part of the study area, the aquifer consists of formations associated with the Maverick Basin, a restricted marine basin situated between the Stuart City reef complexes to the south. Early deposition in the Maverick Basin is characterized by the accumulation of lagoonal evaporites and organic-rich euxenic shales of the West Nueces and McKnight Formations. With time and sediment loading, the Maverick Basin subsided to become a deep open marine basin in which the sediments of the Salmon Peak Formation accumulated. The Salmon Peak Formation is characterized by thick massive lime mudstone, capped by a grainstone that grades into a mudstone.

In the eastern part of the study area, the Maverick Basin sediments interfinger with the synchronous Devils River Formation and terminate to the east against the San Marcos Platform. This formation is informally subdivided into the upper and lower Devils River, with the lower Devils River Formation stratigraphically equivalent to the West Nueces and McKnight Formations and the upper Devils River Formation equivalent to the Salmon Peak Formation. The lower Devils River Formation is characterized by dense, shaley, nodular mudstone that grades to a bioturbated mudstone to wackestone capped by a mudstone and collapsed breccia. The upper Devils River Formation represents carbonate banks of rudist bioherms and biostromes, composed of wackestones and miliolid grainstones.

A series of marine transgressive/regressive sediment cycles ended deposition of the carbonate units of the Maverick Basin and Devils River Formation. These units cap the Edwards aquifer with about 490 meters of confining layers of Del Rio Clay (Upper Cretaceous) and the Indio Formation (Tertiary) predominantly in the central and eastern parts of the Edwards aquifer system.

Scattered throughout Uvalde County also are a series of volcanic to subvolcanic intrusive rocks. The aphanitic to phaneritic ultramafic basalts occur as dikes, plugs, and hypabyssal irregular shaped diatremes within the Edwards aquifer. The age of these intrusions varies from 72 to 80 Ma (Miggins and others, 2004). Recent high-resolution aeromagnetic surveys from 2001 (Smith and others, 2002) detected more than 200 shallow intrusive bodies with only 30 having a surface expression. These mafic diatremes and plugs are hypothesized to act as barriers to groundwater flow and as possible traps for natural gas in the subsurface.

The present-day structure of the Edwards aquifer formed along a crustal zone of weakness known as the Ouachita structural belt. This structural belt is a deep zone of weakness in the Earth's crust which has seen several continental collision and separation episodes since the Precambrian. Superimposed on this ancient belt is the Balcones fault zone, which is a Miocene age, east-west trending zone of normal faults that are downthrown to the south. Notable faults associated with this structural trend in the study area include Cooks, Black Mountain, Blue Mountain, Agape, and Connor faults (fig. 1*B*) (Clark and Small, 1997; and Clark, 2003). The Agape fault is slightly upthrown in relation to the Blue Mountain fault with a graben being formed between the two.

The Uvalde Salient represents a structural high, trending northwest to southeast, which is not associated with faulting splays of the Balcones fault zone. This structural high brings confined units of the Edwards aquifer up from a depth of 275 meters to the surface over a horizontal distance of 14.5 kilometers, then drops the units 92 meters below ground surface over a distance of 9.7 kilometers. The development of this structure is thought to have been synchronus with the emplacement of magma during the late Cretaceous (Ewing and Caran, 1982; Ewing and Barker, 1986) and then modified by Miocene-age faulting.

Hydrologic Setting

Recharge to the Edwards aquifer is mainly attributed to streamflow loss through channel bed infiltration for streams that cross the outcrop area of the Edwards aquifer. Other possible recharge mechanisms to the area include subsurface discharge from the Trinity aquifer, Buda Limestone, Austin Chalk and Leona Gravels; and distributed recharge associated with direct infiltration from precipitation. While the measurement of stream loss across the outcrop belt of the Edwards aquifer can give a limited estimate of recharge in a broad scale, the quantification of other sources of recharge is determined by a water-balance analysis.

In Uvalde County, three contributing watersheds (Frio, Dry Frio, and Nueces Rivers) flow from the northern end of the county into the outcrop belt of the Edwards aquifer. Channel bed infiltration from these rivers is recharged into the aquifer and migrates downdip into the confined region of the aquifer. Green, Bertetti, and others (2006) concluded that there is little contribution of groundwater flow from the western side of Uvalde County because of the presence of a low permeability zone separating higher permeability conditions to the west (the Kinney County "pool") and high permeability zones in the eastern Uvalde County. The southern limit of freshwater flow is associated with the location of the "bad water line" (Shultz, 1994 [1,000 mg/L of total dissolved solids threshold]). The exact structure and position of this transition is not well understood.

Water level altitude data from November 2006 are contoured in figure 2, generally the surface dips downward to the south. Elevations for the potentiometric surface south of the "bad water line" and west of State Road 55 are not provided because of lack of data for those regions. There is a topographic high to the east of the city of Uvalde. This topographic high creates two troughs to the east and west. One trough occurs north of the city of Uvalde, running through the city of Knippa. This trough runs through an area locally referred to as the "Knippa gap," a structure that is a combination of groundwater flow caused by the Uvalde Salient and enhanced permeability associated with localized faulting (Green, Bertetti, and others, 2006). The other trough runs to the south between Blanco Creek and the Sabinal River, northwest of the city of Sabinal, and is not historically associated with known structures. The convergence of these two troughs appears to merge together south of the city of Sabinal and trend southeastward into Medina County.

Sampling

Sample sites were selected from a network of wells associated with the July 2004 water level synoptic conducted by Clark and Journey (2006). The sites included municipal, domestic, agricultural, and several monitoring wells present in the study area. Criteria used for selection of a well for sampling included (a) water production from the freshwater zone of the Edwards aquifer, (b) presence of an operating pump that could be used to sample for dissolved gases, (c) known well construction, (d) known depth and production intervals, and (e) permission of the well operator. Many possible agricultural wells were eliminated from consideration because of lack of use during the time of sampling. Four municipal, four domestic, three monitoring and one agricultural well were selected over an even distribution from up to downgradient within the study area (fig. 1*B*, table 1). Selected wells produce from the Maverick Basin facies (Salmon Peak and McKnight Formations) and the Devils River Formation. The production depth for the wells varied with location from 51 to 369 meters below ground surface. Data collected from two saline zone monitoring wells (East Uvalde 1 and East Uvalde 4) are included in this study. These monitoring wells are included to illustrate the differences between the dissolved gas content and age relations between the freshwater and saline zone transition wells. Samples and geophysical logs from these wells were taken from a prior investigation in the fall and winter of 2002.

Sampling consisted of two techniques depending on the conditions present at the wellhead (table 1). Municipal, domestic, and agricultural supply wells with working pumps installed in the well were sampled directly from a sampling port present at the wellhead. Upon confirmation with the well operator as to pump operation, wells were assumed to be sufficiently purged for sampling. After connecting the sample apparatus to the wellhead port, water was allowed to flow through a multiparameter meter equipped with a flow cell for approximately 5 to 10 minutes. During this initial purging of the sample apparatus, field parameters were measured with a calibrated multiparameter meter equipped with temperature, specific conductance, and pH probes. Upon stabilization of these field parameters, the water was routed through the dissolved gas sample apparatus (an inline copper tube with a back pressure valve). Water flowed through the copper sample tube with a minor back pressure being supplied to the system, to ensure that no bubbles formed in the water sampling stream. The copper tube was sealed at pressure using refrigeration clamps and then removed from the sampling apparatus. After the dissolved gas sample was collected, a tritium sample bottle (250 mL high density polyethylene bottle with polyseal cap) was completely filled and capped, allowing no headspace. A final set of field parameters were recorded to compare the initial measurements and ensure that water quality conditions were stable during sampling.

Monitoring wells with no pumps present were sampled using a discrete interval sampler at selected intervals within the open interval of the well. The wells were first logged to determine zones to be sampled using a portable geophysical logging system. Fluid conductivity, temperature, and fluid pressure readings were logged at 6-inch intervals at a rate of about 3.05 meters per minute for the length of the open borehole (about 152 meters). Specific sampling points were selected for discrete interval sampling on the basis of logs and spacing along the open well intervals. A U.S. Geological Survey- (USGS) developed discrete dissolved gas sampler was attached to the portable logging winch and lowered to the selected depth for sample collection. After acquiring the dissolved gas sample, a 500-mL bulk fluid sampler was then attached to the winch and a similar process was used to obtain enough water for the tritium sample. At the surface, the bulk sampler was open and the contents used to rinse and fill a tritium sample bottle. Since there was little sample water remaining in the bulk fluid sampler, no field parameters were measured for these samples. This process was repeated with successively deeper samples until the sampling was complete.

Laboratory Analysis

Dissolved gas samples were extracted on an ultra-high vacuum extraction line at the USGS Noble Gas Laboratory (USGS NGL) in Denver, Colorado. The gas extracted from the samples was analyzed for nitrogen, oxygen, methane, and argon using a quadrapole mass spectrometer in dynamic operation mode; noble gas isotopic concentrations and compositions (helium, neon, argon, krypton, and xenon) were measured using separate aliquots on a magnetic sector mass spectrometer run in static operation mode. All gas concentrations are reported in units of standard temperature and pressure ([STP] – 0 degrees Celsius [°C] at 1 atmosphere).

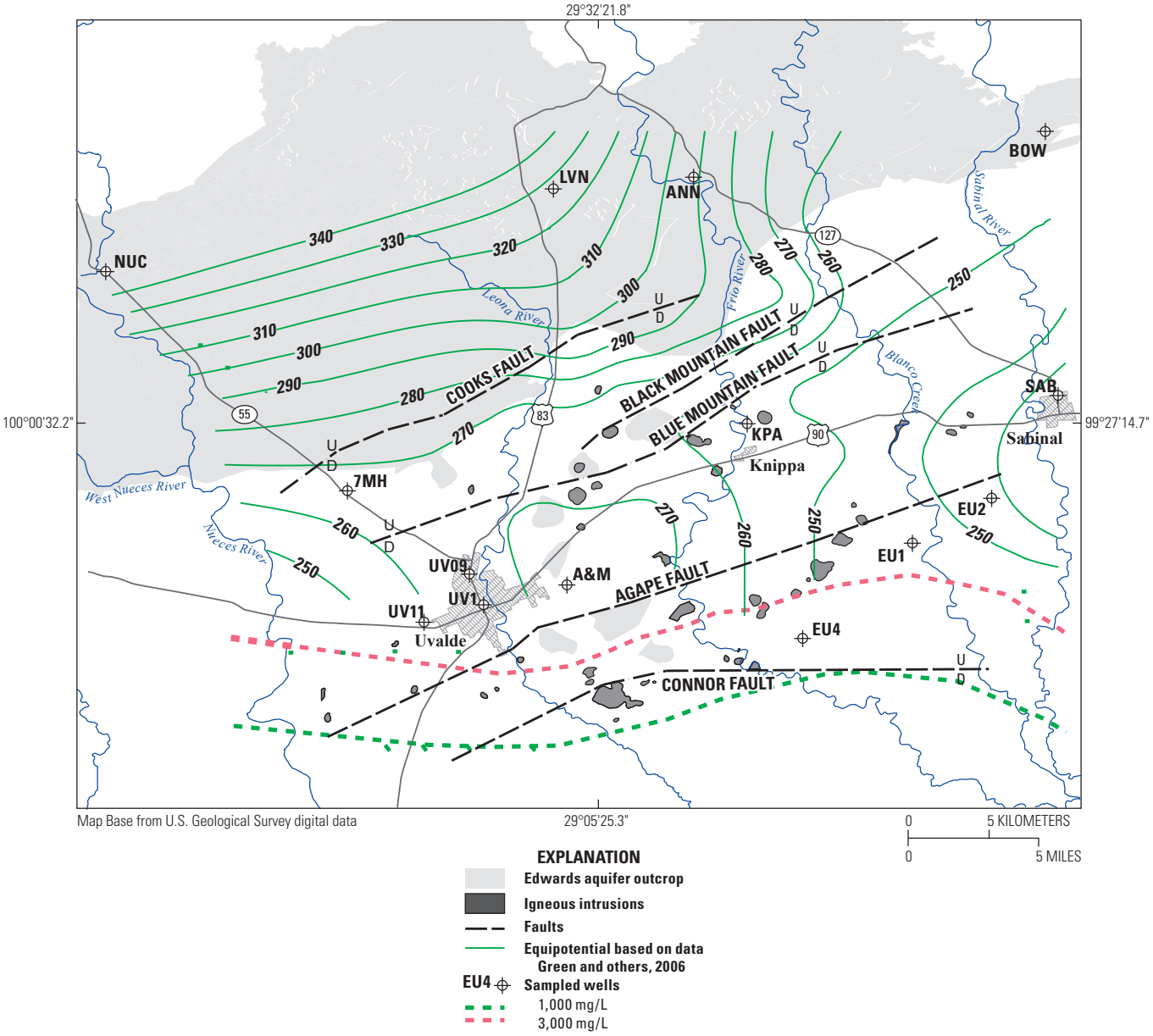

Figure 2. Potentiometric surface of Edwards aquifer water levels as interpreted from data in Green, Bertetti, and others (2006).

Tritium concentrations were measured by the ^{3}He in-growth method (Bayer, Schlosser, and others, 1989; Clark, Jenkins, and Top, 1976). Approximately 170 mL of unfiltered sample water was completely degassed and sealed into a vacuum flask. Tritiogenically produced ^{3}He derived from the degassed sample was allowed to accumulate in the flask for approximately 100 days. The accumulated ^{3}He was extracted and measured using a magnetic sector mass spectrometer and ^{3}H concentration is then calculated using the known decay constant of ^{3}H (Lucas and Unterweger, 2000) and time of accumulation. This procedure results in a lower detection limit of approximately 0.05 tritium units (TU) where 1 TU is equals to one atom of ^{3}H per 10^{18} atoms of hydrogen.

Data Analysis

For the determination of the amount of tritiogenic ^{3}He (^{3}He*) in the dissolved gas phase of a sample, a number of parameters must be defined. Total amount of ^{3}He contained within a sample ($^3He_{measured}$) is a combination of ^{3}He derived from the atmosphere in equilibrium with the groundwater ($^3He_{solubility}$), ^{3}He derived from excess gas trapped during recharge ($^3He_{ea}$) and excess ^{3}He ($^3He_{excess}$) from a combination of ^{3}He released to groundwater from radioactive production in geological materials and (or) an external flux ($^3He_{terr}$), and ^{3}He generated from ^{3}H decay (^{3}He*).

$$^3He_{measured} = {}^3He_{solubility} + {}^3He_{ea} + {}^3He_{excess}$$

where

$$^3He_{excess} = {}^3He_{terr} + {}^3He^*$$

For the solution of the solubility and excess gas components the Closed Equilibrium (CE) model (Aeschbach-Hertig, Peeters, and others, 1999) was used. The CE model uses a chi-squared comparison of modeled to measured dissolved gas data for neon (Ne), argon (Ar), krypton (Kr), xenon (Xe) and nitrogen (N_2) in order to determine recharge temperatures and amounts of excess gas present in waters. The amount of $^3He_{terr}$ is calculated by subtracting the modeled ^4He from the CE-model from ^4He measured concentrations from the samples. The result represents the amount of excess ^4He associated with the terrigenic component. Assuming that the excess helium is a combination of *in-situ* production and an external flux of helium, a $^3He/^4He$ ratio of 2.08×10^{-7} is multiplied by the concentration of excess ^4He to define the amount of $^3He_{terr}$. This ratio of terrigenic helium is measured from tritium absent samples that contained high excess helium concentrations sampled from East Uvalde 4. By subtracting the solubility, excess gas and terrigenic ^3He concentrations from the measured, $^3He^*$ is determined. The apparent groundwater age is defined by the ratio of $^3He^*$ to measured ^3H values and by using a decay constant (λ) of 0.05621 $year^{-1}$ (half-life of 12.32 years) (Lucas and Unterweger, 2000) and the equation:

$$\text{Apparent age (in years)} = 1/0.05621 * \ln (1+{}^3He^*/{}^3H).$$

Results

Geophysical Logs

The geophysical logs obtained prior to sampling of the monitoring wells are presented in Appendix 1. The logs were collected from the open intervals in the monitoring wells Seven Mile Hill, East Uvalde 2, Uvalde Index, East Uvalde 1, and East Uvalde 4.

Electrical Conductance Logs

The electrical conductance of water is defined as its ability to conduct electrical current. The electrical current is a function of the amount of charged ions dissolved in solution (total dissolved solids or TDS); therefore conductivity of a solution is proportional to its TDS. Applying the correlation between TDS concentrations and fluid conductance derived from previous data (TDS [mg/L] = (6.9146 × Specific Conductance [milliSiemens per meter (mS/m)] – 150.02) one can estimate TDS values for the borehole waters in Uvalde County. According to this correlation, a value of 166.3 mS/m correlates with the 1,000 mg/L TDS, the concentration of dissolved solids that distinguishes fresh from saline waters in the Edwards aquifer (Shultz, 1994). The logged monitoring wells have similar conductance values of approximately 47 to 55 mS/m with the exception of increased conductance values in East Uvalde 1 (approximately 70 to 75 mS/m) and East Uvalde 4 (approximately 425 to 450 mS/m) associated with the freshwater/saline water transition zone in the southeastern part of Uvalde County. Though East Uvalde 1 satisfies the condition as a freshwater monitoring well (368 mg/L TDS), conditions present in the well show that this well represents a transitional well between the freshwater zone and saline water zone of the Edwards aquifer.

Temperature Logs

Temperature profiles from the monitoring wells show slightly more variation than the conductance profiles. East Uvalde 2 and Uvalde Index wells have almost no thermal gradient observed (less than 0.5 degrees Celsius per one hundred meters [°C/100 m]) with water temperatures measured between 23.5 °C and 24.5 °C. Seven Mile Hill also has a steep temperature gradient in the upper portion of the well; however, the gradient lessens in the lower 200 feet of the borehole with overall temperatures ranging from 23.0 to 24.0 °C. Both East Uvalde 1 and 4 show significant thermal gradients (1.3 and 2.1 °C/100 m respectively) and temperatures ranging from 29.5 to 35.0 °C. Although the increased temperatures observed in East Uvalde 1 and 4 could be attributed to greater depth when compared to the majority of the freshwater wells (see table 1), a comparison of East Uvalde 1 and 4 temperatures with East Uvalde 2 at similar depths demonstrates an approximate 8 to 10 °C increase associated with East Uvalde 1 and 4.

King and Simmons (1972) calculated the heat flow associated with a deep well in Uvalde County and showed that it was about 46 milliWatts per square meter (mW/m^2) with a thermal gradient of 2.16 °C/100 m. Other sources for thermal gradient data (Woodruff and Foley, 1985) indicate that deep thermal gradients along the Balcones fault zone (in the study) area also range from 2.05 to 2.46 °C/100 m. Assuming that the thermal conductivity is about 2.19 Watts per meter per degree kelvin (W/m/K) for a water-saturated limestone, the calculated heat flow in the study area is fairly constant from about 44.9 to 53.9 mW/m^2. Temperature gradients measured in this investigation range from less than 0.5 °C/100 m in the freshwater wells to 1.3 to 2.1 °C/100 m in the saline-zone transition wells. The thermal and conductance data indicate that the groundwater flow is becoming more stagnant as it moves into the freshwater/saline water transition zone, not only mixing with a high TDS end member, but also coming into thermal equilibrium with the surrounding crustal heat fluxes. A direct result of this interpretation is that there must be a distinct difference in groundwater residence times (groundwater age) associated with the freshwater wells as compared to the saline transition zone wells.

Another example of this broad interpretation can be observed in comparison of the historical geophysical logs from East Uvalde 2 (fig. 3). The logs from November 2002 compared to the logs from November 2005 show a clear change in specific conductance and temperature profiles noted in the well

Table 1. Sample location data.

[mbgs, meters below ground surface; m, meter; not available, data not available for this publication]

Sample	Description	Type of well	State well number	U.S. Geological Survey station number	Depth (mbgs)	Sampled inverval (mbgs)	Production formation	Sample type	Sample date (mm/dd/yyyy)	Figures 1, 2, and 6 symbol
Freshwater zone										
EU2-1187	East Uvalde 2, 362 m	Monitoring	YP-69-44-902	291612099302001	476	362	Devils River Formation	Discrete	11/15/2005	EU2
EU2-1293	East Uvalde 2, 394 m	Monitoring	YP-69-44-902	291612099302001	476	394	Devils River Formation	Discrete	11/15/2005	EU2
EU2-1403	East Uvalde 2, 428 m	Monitoring	YP-69-44-902	291612099302001	476	428	Devils River Formation	Discrete	11/15/2005	EU2
EU2-1503	East Uvalde 2, 458 m	Monitoring	YP-69-44-902	291612099302001	476	458	Devils River Formation	Discrete	11/15/2005	EU2
KPA	City of Knippa, north	Production	YP-69-43-606	291840099382601	213	213	Salmon Peak and McKnight Formations/Devils River Formation	Pumped	11/14/2005	KPA
SAB	City of Sabinal 3	Production	YP-69-45-405	291937099280501	369	369	Devils River Formation	Pumped	11/14/2005	SAB
A&M	Texas A&M AgExt	Agricultural	YP-69-51-114	291417099442901	Not available	172	Salmon Peak and McKnight Formations	Pumped	11/14/2005	A&M
LVN	Livingston	Domestic	YP-69-35-401	Not available	51	Not available	Devils River Formation (upper to middle)	Pumped	02/10/2006	LVN
UV11	City of Uvalde 11	Production	YP-69-50-503	291202099491001	161	161	Salmon Peak Formation	Pumped	11/14/2005	UV11
NUC	Nueces	Agricultural	YP-69-33-701	292346099594701	Not available	Not available	McKnight Formation (minor West Nueces)	Pumped	02/10/2006	NUC
UV09	City of Uvalde 9	Production	YP-69-50-203	291407099473501	160	160	Salmon Peak Formation (near base, possibility of upper McKnight)	Pumped	11/14/2005	UV09
ANN	Annandale	Domestic	YP-69-35-502	292652099401601	82	82	Devils River Formation (middle to lower)	Pumped	02/10/2006	ANN
7MH-130	Seven Mile Hill, 40 m	Monitoring	YP-69-42-709	291623099514401	220	40	Salmon Peak Formation	Discrete	11/17/2005	7MH
7MH-260	Seven Mile Hill, 79 m	Monitoring	YP-69-42-709	291623099514401	220	79	Salmon Peak Formation	Discrete	11/17/2005	7MH
UVI-290	Uvalde Index, 88 m	Monitoring	YP-69-50-302	291237099471201	107	88	Salmon Peak Formation	Discrete	11/16/2005	UVI
UVI-330	Uvalde Index, 101 m	Monitoring	YP-69-50-302	291237099471201	107	101	Salmon Peak Formation	Discrete	11/16/2005	UVI
BOW	Bowman Ranch	Domestic	YP-69-37-402	292711099282201	212	212	Devils River Formation	Pumped	11/17/2005	BOW
Saline-water zone										
EU1-1050	East Uvalde 1, 320 m	Monitoring	YP-69-52-202	291443099325801	457	320	Salmon Peak Formation	Discrete	06/12/2003	EU1
EU1-1140	East Uvalde 1, 348 m	Monitoring	YP-69-52-202	291443099325801	457	348	Salmon Peak Formation (faulted with facies change)	Discrete	06/12/2003	EU1
EU1-1250	East Uvalde 1, 381 m	Monitoring	YP-69-52-202	291443099325801	457	381	Devils River Formation	Discrete	06/12/2003	EU1
EU1-1350	East Uvalde 1, 412 m	Monitoring	YP-69-52-202	291443099325801	457	412	Devils River Formation	Discrete	06/12/2003	EU1
EU1-1470	East Uvalde 1, 448 m	Monitoring	YP-69-52-202	291443099325801	457	448	Devils River Formation	Discrete	06/12/2003	EU1
EU4-1000	East Uvalde 4, 305 m	Monitoring	YP-69-52-404	291133099363801	446	305	Salmon Peak Formation (faulted)	Discrete	06/02/2003	EU4
EU4-1100	East Uvalde 4, 335 m	Monitoring	YP-69-52-404	291133099363801	446	335	Salmon Peak Formation	Discrete	06/02/2003	EU4
EU4-1160	East Uvalde 4, 354 m	Monitoring	YP-69-52-404	291133099363801	446	354	Salmon Peak Formation	Discrete	06/02/2003	EU4
EU4-1300	East Uvalde 4, 396 m	Monitoring	YP-69-52-404	291133099363801	446	396	McKnight Formation	Discrete	06/02/2003	EU4

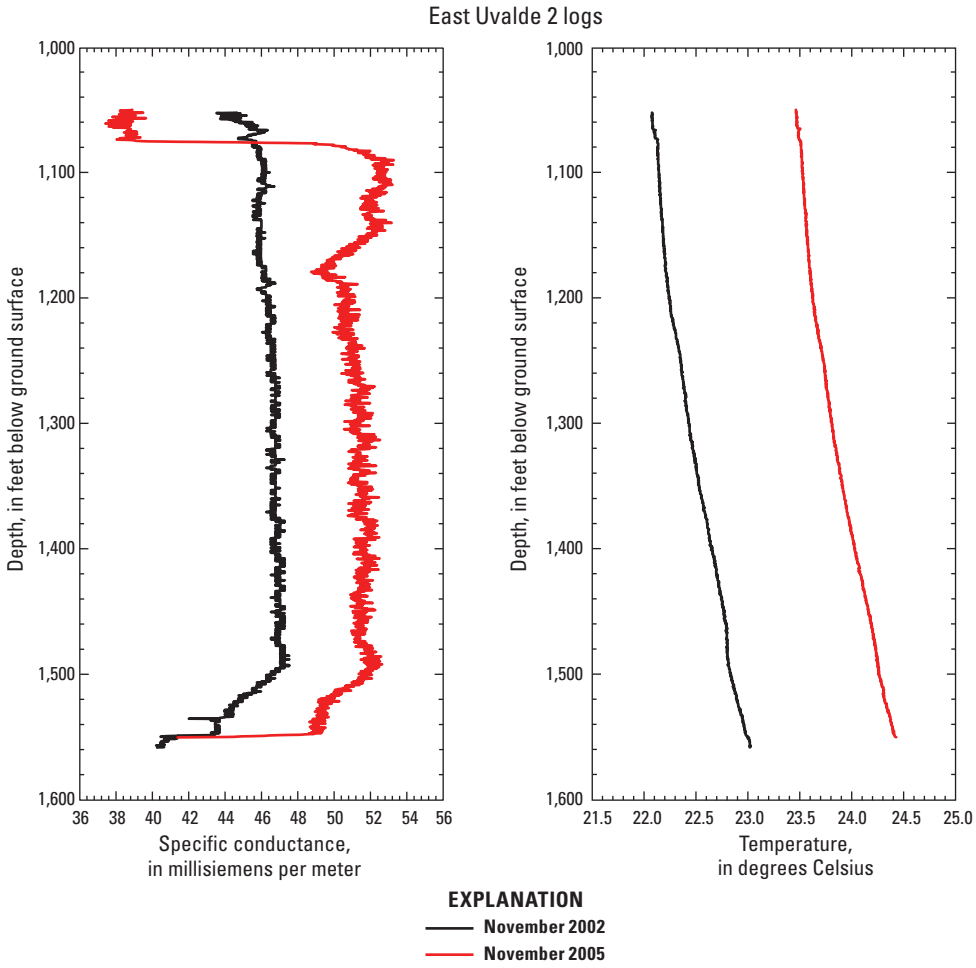

Figure 3. Comparison of geophysical logs of temperature (in degrees Celsius [°C]) and specific conductance (in millisiemens per meter [mS/m]) from monitoring well East Uvalde 2 for November 2002 and November 2005.

between 2002 and 2005. This observation could be indicative of the influx of warmer, more saline water into the freshwater zone of the Edwards aquifer possibly because of increased groundwater withdrawal or low amounts of recharge. More time series data would be required to confirm this hypothesis; however, it demonstrates that the transition zone between the fresh and saline zones in the aquifer is hydraulically connected and is dynamic and the interface responds to change in aquifer use or recharge.

Dissolved Gas in Groundwater

As meteoric water recharges an aquifer and becomes groundwater, it carries a dissolved gas composition that is in equilibrium with the atmosphere. This composition is called air saturated water (ASW) and results from the solubility of atmospheric gas in water while at a fixed temperature, salinity and partial pressure. Although the water is isolated from the atmosphere, the dissolved gas composition is assumed to remain fixed, reflecting conditions at the time of recharge. By measuring the dissolved gas composition of a groundwater sample and applying a solubility model, such parameters as temperature, pressure, and salinity of the recharge conditions can be resolved even though the physical conditions have changed (that is, temperature and salinity) since recharge. This modeling assumes that the gases used must be atmospherically derived, have a homogeneous composition in the atmosphere that does not change with time, have no subsurface sources, and are chemically inert.

Noble Gas Solubility

Noble gases, such as helium, neon, argon, krypton, and xenon represent a wide range of atomic masses and isotopic compositions that are thoroughly characterized in the atmosphere, have well understood thermodynamic and chemical properties, and are chemically inert. Many of the gases (that is, neon-20 and argon-36) have no subsurface sources and are reliable indictors of atmospheric or air saturated water interactions in isolated reservoirs. Other noble gases, like helium-4

and argon-40, have well defined subsurface production mechanisms that allow the qualitative or quantitative interpretation of groundwater age. In general, the solubility of the noble gases is dependent on the atomic mass, with the heavier gases (that is, argon, krypton, and xenon) being more soluble in water than the lighter gases (that is, helium and neon). This difference in solubility that occurs with atomic mass and vastly different partial pressures in the atmosphere produces distinct ratios of the gases in air saturated water which reflect the physical conditions present at the time of equilibrium; therefore, at the time of recharge.

Excess Air

Sometimes the concentrations of the measured dissolved gases are higher than what could be explained from just atmospheric sources. Heaton and Vogel (1981) noted that the composition of the excess gas component (above that of solubility) of a suite of groundwater samples was similar to that of atmospheric composition. The dissolved excess gas in the samples was attributed to the trapping of bubbles of air during recharge and complete dissolution of the bubbles with downward flow and increasing hydrostatic load. This excess gas component is known as excess air.

Later work by Stute and Sonntag (1992), Aeschbach-Hertig, Peeters, and others (1999), and Ballentine and Hall (1999) showed that this excess air component could vary in composition depending on the degree of equilibration of the trapped air and possible loss, fractionating the original air-like component. This type of fraction of the air-like excess component is referred to as the closed equilibrium (CE) model (Aeschbach-Hertig, Peeters, and others, 1999). The CE model assumes that gas equilibration occurs in a closed system between air saturated groundwater and small bubbles being trapped in the quasi-saturated zone (Kipfer, Aeschbach-Hertig, and others, 2002). The free gas component in the quasi-saturated zone has a fixed volume that does not easily exchange with the free unsaturated zone air. Because of relatively slow groundwater velocities and slightly elevated pressure above that of atmospheric, there is a repartitioning of the trapped gas in groundwater, thereby establishing a new equilibrium concentration that is more indicative of the amount of free gas remaining in solution. If all of the free gas is forced into solution, the excess gas component will have an air-like composition (excess air). However, if free gas remains after equilibration, the dissolved excess gas component will be enriched in the more soluble gas components, giving a fractionated excess gas composition that favors the more soluble (greater mass) molecular gases. For implementation of the CE model, measured dissolved noble gas components are compared to modeled concentration values using estimated parameters of temperature, initial concentration of entrapped air (Ae), and the reduction of entrapped volume by dissolution and compression (F), with the assumption that the water was fresh (or low salinity) and the partial pressure of the gases is associated with atmospheric pressure at the elevation of the water table. An error weighted least squares fit is used to solve for free model parameters (T, Ae, and F) by minimizing chi-squared values (X^2).

Measured noble gas compositions (dissolved gas) in cubic centimeters at standard temperature and pressure per gram of water ($cm^3(STP)/g_{H2O}$) for helium (He), neon (Ne), argon (Ar), krypton (Kr), and xenon (Xe), for both the wells in the freshwater and saline-water zones are listed in table 2 along with the dissolved nitrogen (N_2) and methane (CH_4) concentrations. Isotopic compositions of helium (R/R_A, where R is the $^3He/^4He$ of the sample normalized to the atmospheric ratio [R_A] of $^3He/^4He$ [1.384×10^{-6}]), neon ($^{20}Ne/^{22}Ne$) and argon ($^{40}Ar/^{36}Ar$) are also presented in table 2. In general, the concentrations for the conservative atmospherically derived gas components (Ne, Ar, Kr, Xe and N_2) are close to that of air saturated water at 20 °C (305 meters elevation). Because of the lack of subsurface production of ^{20}Ne and ^{36}Ar isotopes, the concentrations of these gases provide insight into parameters involved with recharge and excess atmospheric gas. To further distinguish the atmospheric origin of the waters a binary plot of F $^{20}Ne/^{36}Ar$ values compared to $1/^{36}Ar$ ([$cm^3(STP)/g_{H20} \times 10^{-3}$]) is presented in figure 4*A*. The F value here is defined as the measured $i/^{36}Ar$ (where i is the species of gas in question; for example, N_2, ^{20}Ne, ^4He) of the sample, normalized to $i/^{36}Ar$ of ASW at 20 °C at an elevation of 305 meters. Included on the plot are data for ASW at temperatures of 15 °C, 20 °C and 25 °C, as well as the addition of excess air (unfractionated) and fractionated air associated with a sample of 20 °C ASW at an elevation of 305 meters.

F $^{20}Ne/^{36}Ar$ values greater than one would indicate that there is an increase in the concentration of ^{20}Ne relative to ^{36}Ar. This increase in F $^{20}Ne/^{36}Ar$ values along with decreasing $1/^{36}Ar$ (increasing ^{36}Ar concentration) is an indicator of excess gas above that of the normalizing ratio. A majority of the dissolved gas data falls into this classification (fig. 4*A*). Though there is a subtle variation in the values caused by differences in the recharge temperature and amount of excess air of the sample compared to the normalizing ratio, the general trend is for the majority of the dissolved gas sample to be derived from air equilibrated waters, with some component of excess gas associated with recharge.

One group of samples deviates from this trend. Samples from East Uvalde 4 plot opposite to the trend noted in respect to air saturated waters with excess dissolved gas. The $F^{20}Ne/^{36}Ar$ values are less than one with correspondingly high $1/^{36}Ar$ values. This represents a loss of ^{36}Ar relative to solubility values, along with decreased concentrations of ^{20}Ne relative to ^{36}Ar. The loss of dissolved gas from the system favors the lighter noble gas isotopes relative to 20 °C ASW. The pattern of loss is associated with liquid-gas phase partitioning occurring in the subsurface (Ballentine, Burgess, and Marty, 2002; Bosch and Mazor, 1988). As a parcel of air saturated groundwater comes into contact with a subsurface, free gas phase that contains low concentrations of atmospherically derived noble gas components, new dissolved gas exchange equilibrium within the groundwater will occur to yield a groundwater

Table 2. Dissolved gas compositions with analytical errors.

[NM, not measured; $cm^3(STP)/g_{H2O}$, cubic centimeters per gram at standard temperature and pressure per gram of water; R/R_A, ratio helium-3 to helium-4 normalized to atmospheric helium-3 to helium-4 ratio; ASW 20 °C, 305 meters, air saturated water equilibrated at twenty degrees Celsius at an elevation of 305 meters; ±, plus or minus]

Sample	Helium $cm^3(STP)/g_{H2O}$	±	Neon $cm^3(STP)/g_{H2O}$	±	Argon $cm^3(STP)/g_{H2O}$	±	Krypton $cm^3(STP)/g_{H2O}$	±	Xenon $cm^3(STP)/g_{H2O}$	±	Nitrogen $cm^3(STP)/g_{H2O}$	±	Methane $cm^3(STP)/g_{H2O}$
Freshwater zone													
EU2-1187	8.852E-8	6.1E-10	2.170E-7	5.6E-9	3.330E-4	5.0E-6	7.490E-8	1.5E-9	9.459E-9	2.8E-10	1.371E-2	4.1E-4	<0.002E-02
EU2-1187	7.177E-8	4.9E-10	1.990E-7	5.2E-9	3.396E-4	5.1E-6	7.513E-8	1.5E-9	9.552E-9	2.9E-10	1.411E-2	4.2E-4	<0.002E-02
EU2-1403	6.344E-8	6.3E-10	2.309E-7	6.9E-9	3.423E-4	1.0E-5	7.442E-8	2.2E-9	9.685E-9	2.9E-10	1.441E-2	4.3E-4	<0.002E-02
EU2-1503	6.354E-8	6.4E-10	2.499E-7	7.5E-9	3.345E-4	1.0E-5	7.437E-8	2.2E-9	9.370E-9	2.8E-10	1.376E-2	4.1E-4	<0.002E-02
KPA	6.199E-8	6.2E-10	2.278E-7	8.7E-9	3.392E-4	6.8E-6	7.226E-8	1.4E-9	9.948E-9	2.0E-10	1.412E-2	7.1E-4	<0.002E-02
SAB	8.298E-8	8.3E-10	3.306E-7	7.6E-9	3.920E-4	7.8E-6	7.948E-8	1.6E-9	1.054E-8	2.1E-10	1.763E-2	8.8E-4	<0.002E-02
A&M	5.616E-8	5.6E-10	2.195E-7	7.7E-9	3.324E-4	6.6E-6	7.125E-8	1.4E-9	9.734E-9	1.9E-10	1.372E-2	6.9E-4	<0.002E-02
LVN	1.887E-7	1.9E-9	1.858E-7	5.4E-9	3.013E-4	6.0E-6	6.613E-8	1.3E-9	9.049E-9	1.8E-10	1.229E-2	6.1E-4	<0.002E-02
UV11	6.601E-8	6.6E-10	2.279E-7	4.6E-9	3.238E-4	6.5E-6	6.901E-8	1.4E-9	9.243E-9	1.8E-10	1.344E-2	4.0E-4	<0.002E-02
NUC	5.950E-8	6.0E-10	2.231E-7	4.5E-9	3.384E-4	6.8E-6	7.188E-8	1.4E-9	9.919E-9	2.0E-10	1.381E-2	4.1E-4	<0.002E-02
UV09	5.351E-8	5.4E-10	2.221E-7	4.4E-9	3.202E-4	6.4E-6	6.801E-8	1.4E-9	9.150E-9	1.8E-10	1.312E-2	3.9E-4	<0.002E-02
ANN	4.770E-8	4.8E-10	1.919E-7	3.8E-9	3.461E-4	6.9E-6	7.686E-8	1.5E-9	1.099E-8	2.2E-10	1.325E-2	4.0E-4	<0.002E-02
7MH-130	5.052E-8	5.1E-10	2.189E-7	4.4E-9	3.206E-4	6.4E-6	6.799E-8	1.4E-9	9.125E-9	1.8E-10	1.326E-2	4.0E-4	<0.002E-02
7MH-260	5.120E-8	5.1E-10	2.072E-7	4.1E-9	3.115E-4	6.2E-6	6.498E-8	1.3E-9	8.690E-9	1.7E-10	1.273E-2	3.8E-4	<0.002E-02
UVI-290	5.799E-8	5.8E-10	2.253E-7	4.5E-9	3.128E-4	6.3E-6	6.388E-8	1.3E-9	8.329E-9	1.7E-10	1.296E-2	3.9E-4	<0.002E-02
UVI-330	5.745E-8	5.7E-10	2.238E-7	4.5E-9	3.122E-4	6.2E-6	6.490E-8	1.3E-9	8.391E-9	1.7E-10	1.527E-2	4.6E-4	<0.002E-02
BOW	8.390E-8	8.4E-10	3.311E-7	6.6E-9	3.862E-4	7.7E-6	7.805E-8	1.6E-9	1.038E-8	2.1E-10	1.854E-2	9.3E-4	<0.002E-02
Saline-water zone													
EU1-1050	2.028E-6	1.5E-8	1.752E-7	3.5E-9	3.016E-4	6.0E-6	NM		NM		1.487E-2	4.5E-4	<0.002E-02
EU1-1140	1.511E-6	2.2E-8	2.139E-7	4.3E-9	2.971E-4	5.9E-6	NM		NM		1.464E-2	4.4E-4	<0.002E-02
EU1-1250	2.154E-6	2.0E-8	1.786E-7	3.6E-9	3.238E-4	6.5E-6	NM		NM		1.534E-2	4.6E-4	<0.002E-02
EU1-1350	2.164E-6	2.2E-8	1.778E-7	3.6E-9	2.917E-4	5.8E-6	NM		NM		1.439E-2	4.3E-4	<0.002E-02
EU1-1470	2.351E-6	2.4E-8	2.127E-7	4.3E-9	3.333E-4	6.7E-6	NM		NM		1.627E-2	4.9E-4	<0.002E-02
EU4-1000	3.070E-5	3.1E-7	1.473E-7	2.9E-9	3.010E-4	6.0E-6	NM		NM		1.449E-2	4.3E-4	<0.002E-02
EU4-1100	3.201E-5	3.2E-7	1.443E-7	2.9E-9	2.727E-4	5.5E-6	NM		NM		1.372E-2	4.1E-4	<0.002E-02
EU4-1160	3.419E-5	3.4E-7	1.429E-7	2.9E-9	2.835E-4	5.7E-6	NM		NM		1.400E-2	4.2E-4	<0.002E-02
EU4-1300	3.214E-5	3.2E-7	1.371E-7	2.7E-9	2.789E-4	5.6E-6	NM		NM		1.409E-2	4.2E-4	<0.002E-02
ASW 20°C, 305 meters	4.311E-8		1.783E-7		3.004E-4		6.709E-8		9.165E-9		1.148E-2		

Table 2. Dissolved gas compositions with analytical errors.—Continued

[NM, not measured; $cm^3(STP)/g_{H2O}$, cubic centimeters per gram at standard temperature and pressure per gram of water; R/R_A, ratio helium-3 to helium-4 normalized to atmospheric helium-3 to helium-4 ratio; ASW 20 °C, 305 meters, air saturated water equilibrated at twenty degrees Celsius at an elevation of 305 meters; ±, plus or minus]

Sample	$\frac{R}{R_A}$	±	$\frac{^{20}Ne}{^{22}Ne}$	±	$\frac{^{40}Ar}{^{36}Ar}$	±
			Freshwater zone			
EU2-1187	0.813	0.006	9.862	0.049	294.8	2.9
EU2-1293	1.023	0.008	9.846	0.049	295.1	3.0
EU2-1403	1.008	0.005	NM	0.000	296.7	3.0
EU2-1503	0.991	0.005	9.914	0.050	299.4	3.0
KPA	1.002	0.008	9.867	0.049	294.1	2.9
SAB	1.068	0.009	9.852	0.049	295.5	3.0
A&M	1.035	0.008	9.893	0.049	293.4	2.9
LVN	0.348	0.005	9.846	0.049	295.2	3.0
UV11	1.068	0.009	9.883	0.049	294.1	2.9
NUC	0.983	0.008	9.860	0.049	294.0	2.9
UV09	1.105	0.009	9.904	0.050	295.6	3.0
ANN	0.973	0.008	9.922	0.050	295.5	3.0
7MH-130	1.043	0.008	9.894	0.049	294.0	2.9
7MH-260	1.085	0.009	9.901	0.050	293.6	2.9
UVI-290	1.119	0.009	9.848	0.049	295.1	3.0
UVI-330	1.127	0.009	9.835	0.049	294.6	2.9
BOW	1.042	0.008	9.834	0.049	295.6	3.0
			Saline-water zone			
EU1-1050	0.175	0.005	9.883	0.050	299.7	3.0
EU1-1140	0.184	0.005	9.904	0.049	298.7	3.0
EU1-1250	0.182	0.005	9.888	0.049	300.0	3.0
EU1-1350	0.174	0.005	9.883	0.049	299.0	3.0
EU1-1470	0.178	0.005	9.886	0.049	297.8	3.0
EU4-1000	0.178	0.005	9.890	0.049	302.6	3.0
EU4-1100	0.187	0.005	9.900	0.050	302.0	3.0
EU4-1160	0.195	0.005	9.888	0.049	302.7	3.0
EU4-1300	0.190	0.005	9.917	0.050	301.2	3.0
ASW 20°C, 305 meters	0.980		9.800		295.5	

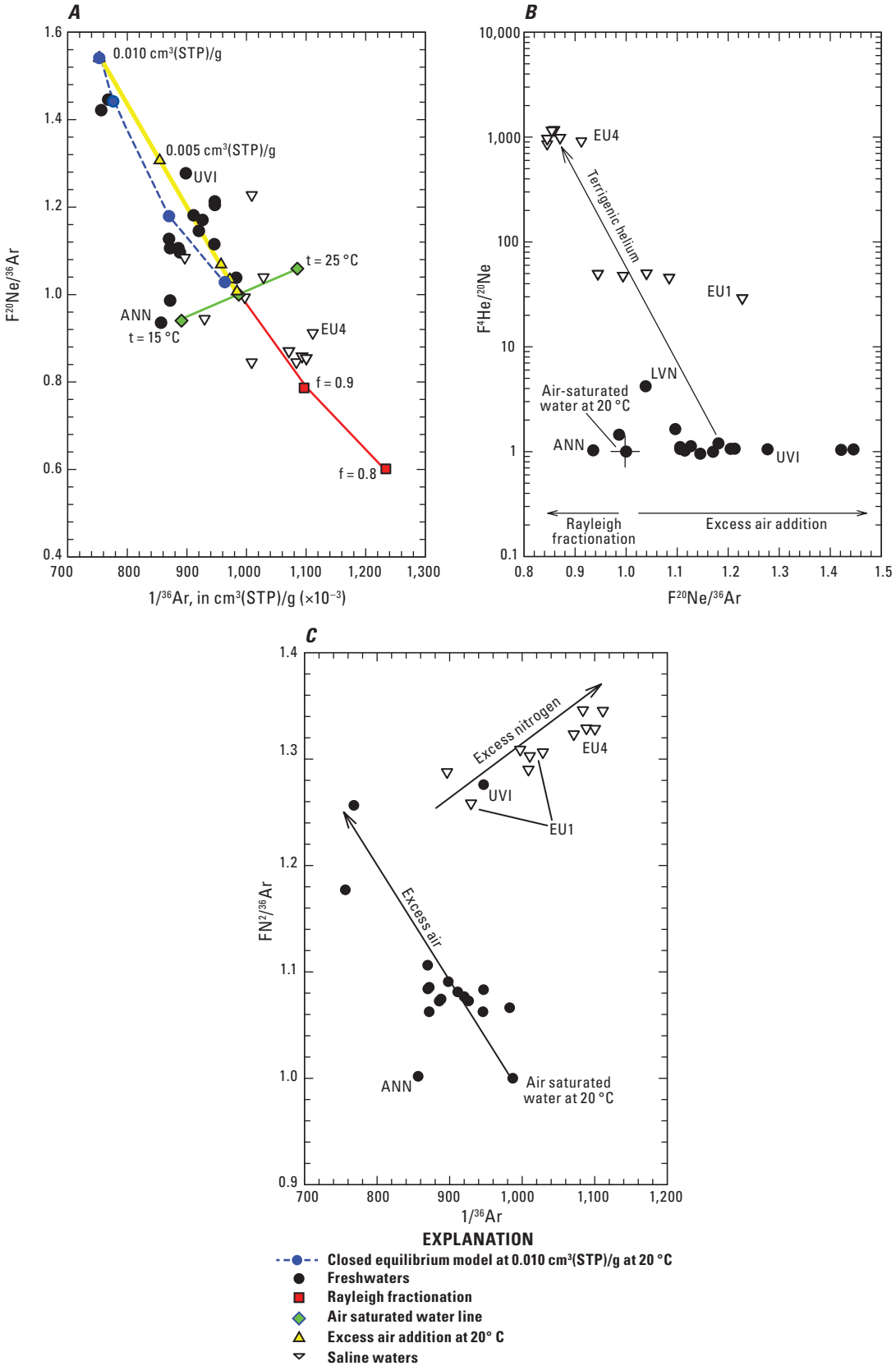

Figure 4. Binary plots of *A*, F $^{20}Ne/^{36}Ar$ compared to $1/^{36}Ar$; *B*, $F^4He/^{20}Ne$ compared to $F^{20}Ne/^{36}Ar$; and *C*, $FN_2/^{36}Ar$ compared to $1/^{36}Ar$. F values are defined as the concentration of gas species i of the sample divided by the concentration of ^{36}Ar of the sample normalized to $i/^{36}Ar$ of air saturated water at a temperature of 20 degrees Celsius (°C) and altitude of 305 meters above sea level. Concentration values for ^{36}Ar are presented in cubic centimeters at standard temperature and pressure per gram of water multiplied by 0.001 ($cm^3(STP)/g_{H2O} \times 10^{-3}$).

depleted in gas relative to its original atmospheric equilibrated value. Solubility relations fractionate the dissolved gases in the groundwater with the lighter, less soluble gases partitioned into the free gas phase and the heavier, more soluble gases tending to remain in the liquid phase. Presented on the plot is a simple Rayleigh fractionation model (Ballentine, Burgess, and Marty, 2002) to show the effects of gas partitioning. The fractional value (f) for the Rayleigh model presented represents the fraction of ^{36}Ar left in solution. The model predicts that approximately 8 percent of the original ^{36}Ar has been lost; however, this could be much greater if the starting gas concentration for the model contained excess atmospheric gases. The exact mechanism that is causing the atmospheric-derived gases to partition out of solution is unclear.

Further evaluation of the dissolved gas compositions with respect to He and N_2 concentrations are presented in figures 4*B* and *C*. The binary plots of F ^{4}He/^{20}Ne versus F ^{20}Ne/^{36}Ar (fig. 4*B*) and F N_2/^{36}Ar versus 1/^{36}Ar (fig. 4*C*) illustrate gas partitioning and addition of excess air to the samples. The F ^{4}He/^{20}Ne value for ^{4}He is coupled with ^{20}Ne and not ^{36}Ar, in order to match the similar solubility of He and Ne.

For both plots (fig. 4*B* and 4*C*) the freshwater data correlate with the excess air trend while the saline waters trend away from assumed atmospheric values. In the F N_2/^{36}Ar compared to 1/^{36}Ar plot, saline water data show an increasing F N_2/^{36}Ar value (N_2 increasing relative to ^{36}Ar) while the 1/^{36}Ar increases. This trend is not predicted by liquid-gas phase partitioning, where the F N_2/^{36}Ar should decrease with decreasing quantities of ^{36}Ar. The trend is interpreted as an addition of excess N_2 above solubility, excess air, and the liquid-gas phase partitioning.

The same excess gas addition is also observed in the He data. The F ^{4}He/^{20}Ne increases as the F ^{20}Ne/^{36}Ar decreases, and reveals a source of excess ^{4}He associated with the saline waters. This excess He is called terrigenic He. The measured concentration of terrigenic He increases to almost 1,000 times that of the atmospheric solubility values, with a homogeneous isotopic composition of 0.19 R/R_A (table 2). Terrigenic He generation in the crust is dominated by ^{235}U, ^{238}U and ^{232}Th decay chain alpha-production but also can be coupled with a flux of helium from the planetary interior. The increase of He with time in groundwaters has been studied as a means of dating young groundwaters (Marine, 1979; Mazor and Bosch, 1992; Solomon, Hunt, and Poreda, 1996; Torgersen and Clarke, 1985; Torgersen and Ivey, 1985). The relative contributions from each source can vary greatly, producing distinctive helium isotopic compositions and variable helium accumulation rates in an area.

Excess N_2 and terrigenic He correlate with groundwater salinity. The strong correlation may be associated with a uniform reservoir of terrigenic He and N_2 (crustally derived N_2) in the saline zone, while variations in the concentration are the result of mixing along the transition zone. While East Uvalde 4 has a fairly uniform gas composition, data suggest that samples from East Uvalde 1 represent a mixing between the fresh and saline waters. The saline waters are characterized by the uniform composition of atmospherically derived water that experienced some liquid-gas phase partitioning and are enriched in terrigenic He and excess N_2 while the freshwaters are constrained by solubility concentrations associated with air saturated waters with some additional dissolved gas component entrained during recharge.

The mixing of fresh and saline waters, as well as the presence of fractionated dissolved gas components, prohibit the application of the CE model to determine the recharge conditions that are associated with the saline and saline transition zone wells. The presence of excess N_2, which correlates with terrigenic helium, suggests that an external flux of He and N_2 dominates the saline zone. The concentrations of terrigenic helium are high enough to indicate that the saline zone waters are much older than modern groundwaters. The thermal data obtained corroborate this postulate that the age of the saline waters is greater than the fresh water. Typical estimates of He crustal flux with production for the area would generate apparent groundwater ages on the order of hundreds to thousands of years for the saline zone. Apparent ages based on ^{4}He concentration are heavily model dependent and are beyond the scope of this report.

Almost all of the freshwater samples plot well with ASW and excess gas concentrations except LVN, UVI-330 and ANN (fig. 4*A*, *B* and *C*). LVN has a minor amount of terrigenic ^{4}He that is not associated with excess N_2, UVI-330 has excess N_2 not associated with terrigenic He, and ANN does not plot well with the rest of the data. The data anomalies from ANN are explained as a difference in recharge temperature that is lower than 20 °C ASW (normalizing ratio for the F value [CE model]). The excess N_2 in UVI-330 can be attributed to denitrification of dissolved nitrogen compounds in the groundwater, but LVN concentration of excess He is more complex. The LVN sample plots as atmospheric-equilibrated groundwater with a slight amount of excess air, but the amount of excess helium observed in the sample cannot be explained by solubility and recharge conditions alone. The sample may be a mix between modern and premodern groundwaters, with the premodern component containing excess He. This important mixing relation can be further defined more clearly by measuring the concentration of ^{3}H in the sample.

Calculated Recharge Temperatures

The calculated recharge temperatures along with values of Ae and F parameters from the CE model (Aeschbach-Hertig and others, 1999) and the X^2 value for the fit test are presented in table 3 for the samples from the freshwater zone. All samples met the criteria for appropriateness of fit of the X^2 test with X^2 values of less than four. Ae values all seem reasonable except for EUV2-1293 which has an extremely high Ae value of 0.147 cm^3 (STP)/g_{H2O} associated with high F value of 0.870. The derived recharge temperature from EUV2-1293 is similar to others sampled at the same time and may possibly represent a sampling problem that is corrected through application of the CE model.

Table 3. Closed equilibrium model parameters and apparent age data.

[$cm^3(STP)/g_{H2O}$, cubic centimeters per gram at standard temperature and pressure per gram of water; *, error is calculated by instrumental error of helium and tritium measurements; **, not calculated; --, no error calculated; <0.5, less than 0.5; Ae, initial concentration of trapped air; F, fractional reduction of entrapped volume by dissolution and compression; TU, tritium unit, °C, degrees Celsius, <0.13, less than 0.13]

Sample	Recharge temperature (°C)	Ae $cm^3(STP)/g_{H2O}$	F	χ^2	Tritiogenically derived helium-3 (TU)	±	Tritium (TU)	±	Apparent age (years)	Recharge date (year)	Error* (years)	Excess helium-4 ($\times 10^{-9}$) $cm^3(STP)/g_{H2O}$
Freshwater zone												
EU2-1187	19.3	0.018	0.735	3.53	8.12	0.28	1.94	0.04	29.3	1977	0.7	35.7
EU2-1293	20.0	0.147	0.870	3.25	12.05	0.29	1.76	0.04	36.7	1969	0.6	22.6
EU2-1403	19.7	0.018	0.645	0.28	3.83	0.28	1.76	0.04	20.6	1985	1.1	6.5
EU2-1503	20.1	0.005	0.202	1.90	0.21	0.28	1.45	0.03	2.4	2004	3.5	<0.5
KPA	18.5	0.005	0.364	0.67	2.95	0.31	2.39	0.05	14.3	1992	1.2	5.2
SAB	18.1	0.010	0.134	2.01	3.46	0.45	2.11	0.04	17.3	1989	1.7	<0.5
A&M	18.8	0.003	0.207	0.41	2.20	0.29	2.32	0.05	11.8	1994	1.3	1.5
LVN	20.7	0.000	0.044	0.11	<0.5	0.45	2.50	0.05	<0.5	2006	--	143.2
UV11	20.6	0.003	0.014	0.09	6.91	0.36	1.98	0.04	26.7	1979	0.9	8.5
NUC	18.3	0.003	0.122	1.09	1.64	0.29	2.00	0.04	10.7	1995	1.7	3.8
UV09	20.7	0.003	0.217	3.29	3.34	0.30	2.49	0.05	15.1	1991	1.1	<0.5
ANN	14.4	0.000	0.204	1.58	0.58	0.23	3.00	0.06	3.2	2003	1.3	1.9
7MH-130	21.3	0.007	0.525	0.17	1.71	0.27	2.27	0.05	10.0	1996	1.4	<0.5
7MH-260	23.2	0.016	0.750	0.62	2.83	0.28	2.13	0.04	15.1	1991	1.2	<0.5
UVI-290	25.9	0.020	0.650	0.82	5.05	0.33	2.56	0.05	19.4	1987	0.9	1.6
UVI-330	24.7	0.012	0.587	0.00	4.97	0.33	2.12	0.04	21.5	1984	1.0	1.0
BOW	18.6	0.008	0.000	0.62	0.75	0.44	2.64	0.05	4.5	2001	2.7	<0.5
Saline-water zone												
EU1-1050	**						0.64	0.02	**	**		
EU1-1140	**						0.21	0.02	**	**		
EU1-1250	**						<0.13		**	**		

The average recharge temperature of the area is 19.8 plus or minus 2.3 °C, which correlates well with the mean annual temperature of 20 °C for Uvalde County. This matches the concept that noble gas recharge temperatures are closely associated with mean annual air temperatures (soil temperatures) for a geographic area (Mazor, 1993; Stute and Sonntag, 1992). The only outlier for recharge temperature is the sample ANN. The computed recharge temperature for the well is consistent with the relations derived from dissolved gas concentration plots (fig. 4*A*, *B*, and *C*), but the measured temperature is six degrees lower than what would be expected for the area. ANN is located in the recharge zone of the Edwards aquifer and is closely associated with the Frio River watershed (fig. 1*B*). The measured recharge temperature is close to that of average air temperatures for February in Uvalde County (13 °C), which coincides with the time the well was sampled. This extremely low recharge temperature can be explained by the hydraulic connection of the well to the Frio River. A close hydraulic connection to the river would cause the noble gas temperatures (NGT) data to mimic the seasonal temperature fluctuation observed in the river. This hydraulic connection would imply that the groundwater age from the well should be on the order of days to weeks. If ANN is not considered, the average recharge temperature of 20.2 plus or minus 1.9 °C is observed.

Tritium Data and Apparent Age

Tritium data are presented in table 3; concentrations are given in tritium units (TU, 1 TU is defined as 1 atom of ^{3}H per 10^{18} atoms of H). All of the freshwater samples contain ^{3}H, as do two samples of the upper zone of East Uvalde 1, while the remaining samples in East Uvalde 1 and East Uvalde 4 have less than 0.05 TU (^{3}H dead). The range of ^{3}H values in the freshwater samples is narrow, because of a combination of low ^{3}H input in precipitation during the last 15 years and the normal decay of ^{3}H associated with residence time. Tritium by itself could be used to quantitatively date the groundwaters using a known input curve (International Atomic Energy Agency, 2004). Because of the narrow range in concentration of recent data and low levels of ^{3}H input, the error associated with such a method is too large to be useful. By definition the freshwaters are classified as modern (if less than 60 years in age) and the ^{3}H dead samples as premodern. This simple classification cannot account for mixing of older tritium dead components into modern waters.

The dissolved gas data from East Uvalde 1 coupled with the tritium data support the interpretation that the samples represent a mixing along the transition zone between the freshwater and saline water zones of the Edwards aquifer. The presence of tritium in the upper samples of the well show that there is a modern component mixing with the premodern component as characterized by high excess He concentrations. The exact degree of mixing is difficult to define though it was observed from historical geophysical log data. There are no end members to determine the scale of mixing beyond saying that a mix between two waters of different apparent ages is occurring.

Apparent ^{3}H-^{3}He Age

Using recharge conditions computed from the CE model and subtracting excess helium component with an isotopic composition of 0.15 R/Ra, the amount of tritiogenically derived ^{3}He ($^{3}He^{*}$) is calculated (table 3). For samples from East Uvalde 1 and East Uvalde 4 monitoring wells, no $^{3}He^{*}$ is calculated for the data. The excess He values in these samples were too high to make an accurate determination of $^{3}He^{*}$ (within the analytical precision of this procedure) and the dissolved gas compositions do not allow the application of the CE model. The $^{3}He^{*}$ values are presented as TU units for ease of apparent age calculation. Unlike the tritium data, there is a wide range in $^{3}He^{*}$ concentrations because of a wide distribution in apparent ^{3}H-^{3}He ages. The amounts of $^{3}He^{*}$ ranging from less than 0.5 TU in LVN to 12.05 TU in EU2-1293.

Calculated apparent ages range from less than 0.5 years to a maximum of 36.7 years for the samples that contain $^{3}He^{*}$, which corresponds to calendar ages of 2006 to 1971. One way to evaluate the validity of the dataset is to plot the value of ^{3}H plus $^{3}He^{*}$ (original ^{3}H concentration in initial recharge) compared to the recharge year of the sample and known ^{3}H input values for the region. Historical ^{3}H concentrations in precipitation from the Waco, Texas dataset of the International Atomic Energy Agency (2004) have compiled a full set of ^{3}H input curves for the United States. Plotted in figure 5 is the average historical ^{3}H input curve and the ^{3}H plus $^{3}He^{*}$ values and associated recharge year for the sample dataset. The data correlate well to the historical input curve, with only five samples plotting significantly below the input curve, implying $^{3}He^{*}$ and ^{3}H are lower than expected in these samples. This finding can be explained by a dilution of the groundwater with a premodern component that contains low to no initial concentrations of ^{3}H. This premodern water dilutes the $^{3}He^{*}$ and ^{3}H concentrations, while the $^{3}He^{*}/^{3}H$ ratio of the sample preserves the age of the modern component. Samples UV11, EU2-1187, EU2-1293, EU2-1503 and LVN plot below the inferred ^{3}H input curve. The historical input curve has some amount of variation associated with different sources of precipitation which contain different ^{3}H concentration within each year, but these five samples show definitive trends away from the expected variation of young or old samples.

The implication for mixing of groundwaters from East Uvalde 2 and East Uvalde 1 is expected. The proximity of the wells to the freshwater/saline water transition zone coupled with our understanding of the dissolved gas data and mixing relations noted in East Uvalde 1, allows us to predict some form of mixing between the modern and premodern components. Unlike the mixing noted in East Uvalde 1, the samples

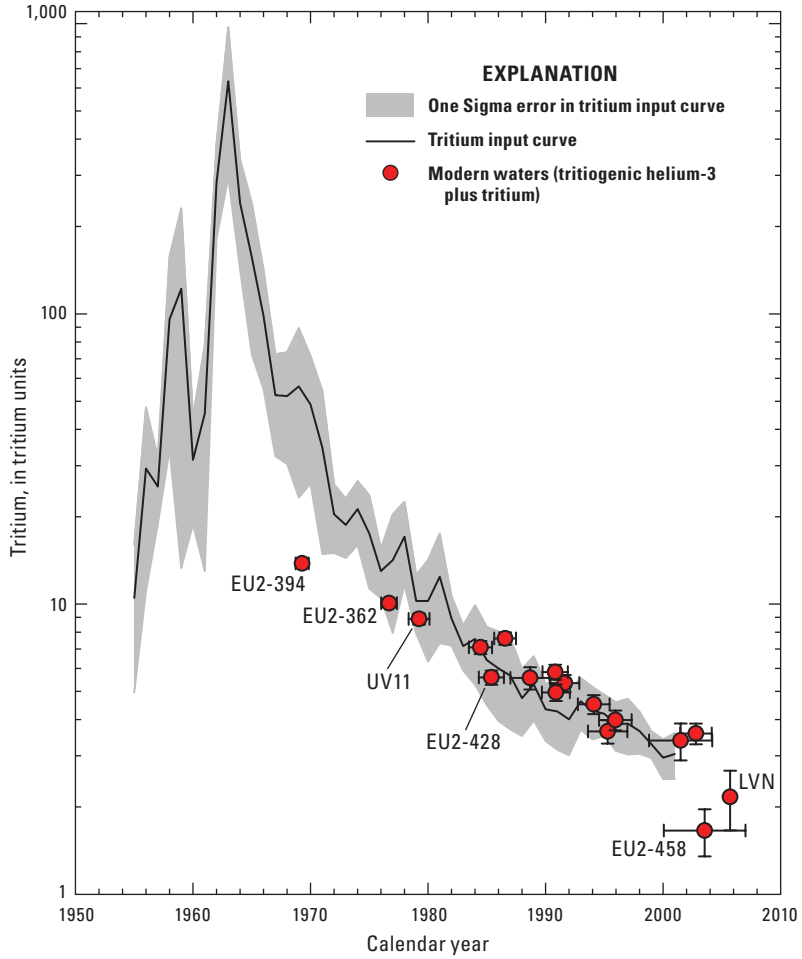

Figure 5. Binary plot of $^{3}H+^{3}He^{*}$ (tritium units) for samples compared to the recharge year from the ^{3}H-^{3}He age, superimposed on the historical ^{3}H input curve from Michel (2007). A one Sigma error (shaded area surrounding the ^{3}H average curve) is reported for the ^{3}H historical data as representing the variation of ^{3}H for an individual calendar year (January through December).

EU2-1186, EU2-1293, EU-1503 and UV11 do not contain high amounts of excess He. The amount of excess He ranges from less than 0.5 to 35.7 (cm^{3}(STP)/g × 10^{-9}) (table 3). The amount of excess He does not correlate with salinity, unlike the correlation mixing observed in East Uvalde 1. The mixed end members for these samples could be derived from modern waters mixing with premodern waters that are not associated with the freshwater/saline-water interface. The premodern end member may be associated with younger, fresher waters than those currently found in the saline zone, but would have long flow paths (mean residence times greater than 60 years) in the freshwater zone of the Edwards aquifer. The longer flow paths would still eventually merge with a modern freshwater system along the freshwater/saline-water transition zone, generating a mixing zone of relatively freshwater of varying apparent ages.

The sample plots are just slightly less than what is expected for recent ^{3}H input and could represent seasonal variability in ^{3}H input values; however, the LVN sample also contains elevated amounts of excess He (143.2 µcm^{3}/kg). LVN was sampled from the midpart of the recharge zone of the Edwards aquifer. The apparent age of the sample was less than 0.5 years and correlates well with the conceptual understanding that young waters are recharging along the outcrop area of the Edwards aquifer. The amount of excess He measured in the sample must be associated with premodern end member. This mixing pattern could be attributed to an unknown interaction between the Edwards and Trinity aquifers. Groundwaters recharged in the Trinity aquifer are assumed to have a longer residence time (tritium dead and some amount of excess He) than those associated with the groundwaters within the recharge zone (ASW He concentrations and modern ^{3}H).

Similar to findings from East Uvalde 2, the mixing of the two component waters produce a sample with a modern apparent age (measurable ^{3}H) but contain appreciable amounts of excess He. The amount of premodern water associated with the LVN sample is difficult to quantify with just the ^{3}H-^{3}He data set because of the low concentrations and uncertainties in the ^{3}H input curve. The assumption that the premodern component is derived from the Trinity aquifer is circumstantial in nature and would need to be tested with more samples from the Trinity aquifer to further substantiate this observation.

Vertical Apparent Age Distribution

As water recharges an aquifer, it displaces earlier recharged waters away from the recharge zone. Apparent age also reflects this displacement of groundwater movement. The apparent age distribution of a set of vertically sampled groundwater samples will reflect the amount of recharge entering an aquifer for a specific area. Normal age distributions should increase with respect to apparent age with depth in an aquifer. The amount of water recharging the system can be quantified using simple models that described aquifer characteristics and the vertical distribution in apparent ages (Vogel, 1967; Solomon, Poreda, and others, 1995). Several wells were selected for multiple samples from different vertically distributed zones in the study area in an attempt to define the magnitude and distribution of groundwater recharge for this area.

The sampling results from the monitoring wells were problematic. Sampling from Seven Mile Hill encountered an obstruction at 353 feet below ground surface that limited data to two intervals. The short screened interval of Uvalde Index limited the number of possible samples to be taken. Only East Uvalde 2 had at least 4 samples taken from different depths.

The results from both Seven Mile Hill and Uvalde Index show increasing apparent age with increasing depth. Calculating the average linear velocity of the groundwater from the change in vertical distance with each sample along with the change in apparent age derives 8.6 meters per year (m/yr) downward for Seven Mile Hill and 5.1 m/yr downward for Uvalde Index. The downward velocity from these two wells does not reflect the downward velocity at the location of the wells, but is linked to the average linear velocity retained when the groundwaters were originally recharged in the aquifer. A conservative estimate of the amount of recharge it would take to generate this apparent vertical velocity is between 1.53 and 2.58 m/yr (assuming 0.3 for porosity of the aquifer and the vertical velocity component represents the velocity of recharging water). This amount of water far exceeds the annual precipitation for the area (approximately 0.60 m/yr), as such, it must be related to a point source infiltration as a significant driving factor for recharge to the system. To understand this finding in detail, more data are needed to fully quantify recharge estimates.

The East Uvalde 2 data are slightly more problematic. Apparent age initially increases with depth for the upper two samples from the well (25.6 to 35.4 years), the apparent ages reverse and begin to decrease in age to an apparent age of 1.2 years at the bottom of the well. In principle, this effect of reversed age gradients could be happening hydraulically in the system, but is improbable in porous media interpretation. Implying a karst conceptual model of driving young water below the older water in the confined aquifer could explain the results. This explanation is problematic in explaining the observed heat flow from the geophysical logs but cannot be ruled out. Another explanation can be that there is vertical flow in the well itself. The ^{3}H-^{3}He data showed that there was mixing of modern and premodern components associated with the two upper samples, but this was not observed in the two deeper samples. Other evidence that further clouds the interpretation of the data is the existence of excess He in the upper two samples which diminishes to no detectable excess He in the bottom of the hole. This pattern in the dissolved gas data and ^{3}H concentrations may be a result of vertical mixing of the groundwaters within the annulus of the well. Mixed modern and premodern waters containing a small amount of excess He and ^{3}H can be mixing with a premodern, fresh component with no excess He in the lower part of the well. The ^{3}H remains in the annulus while the excess He diffuses into the aquifer in the upper portion of the well. This would effectively separate the $^{3}He^{*}$ and ^{3}H giving a false apparent age that would decrease with greater amount of ^{3}He loss. Apparent age interpretation for this well should be questioned.

Apparent Age and Flow Patterns

Apparent age distribution across the study area generally follows a consistent pattern with the youngest samples coming from the recharge zone of the Edwards aquifer and the older samples associated with the confined section of the aquifer. From the four samples in the recharge zone, the apparent age distribution is from less than 0.5 years to 10.9 years and within the confined zone age ranging from 10 to 34.7 years.

A contour of the age data is superimposed on the groundwater flow vectors obtained from the dataset in figure 2. The apparent age contour is constructed from the pumped samples, as well as the uppermost sample taken from the discretely sampled monitoring wells (fig. 6). Figure 6 shows the relations between the apparent age data and assumed groundwater flow pattern in a regional context. Vectors from the potentiometric surface should parallel apparent age gradients, indicating that the longer the flow path, the longer the residence time, and the older the water.

One notable feature within the age contour is a trend of young apparent ages along the axis of the Uvalde Salient. Apparent ages from samples LVN and A&M generate a ridge of young groundwater in the contour that runs in a north-south trend. This incursion of younger water with the salient may

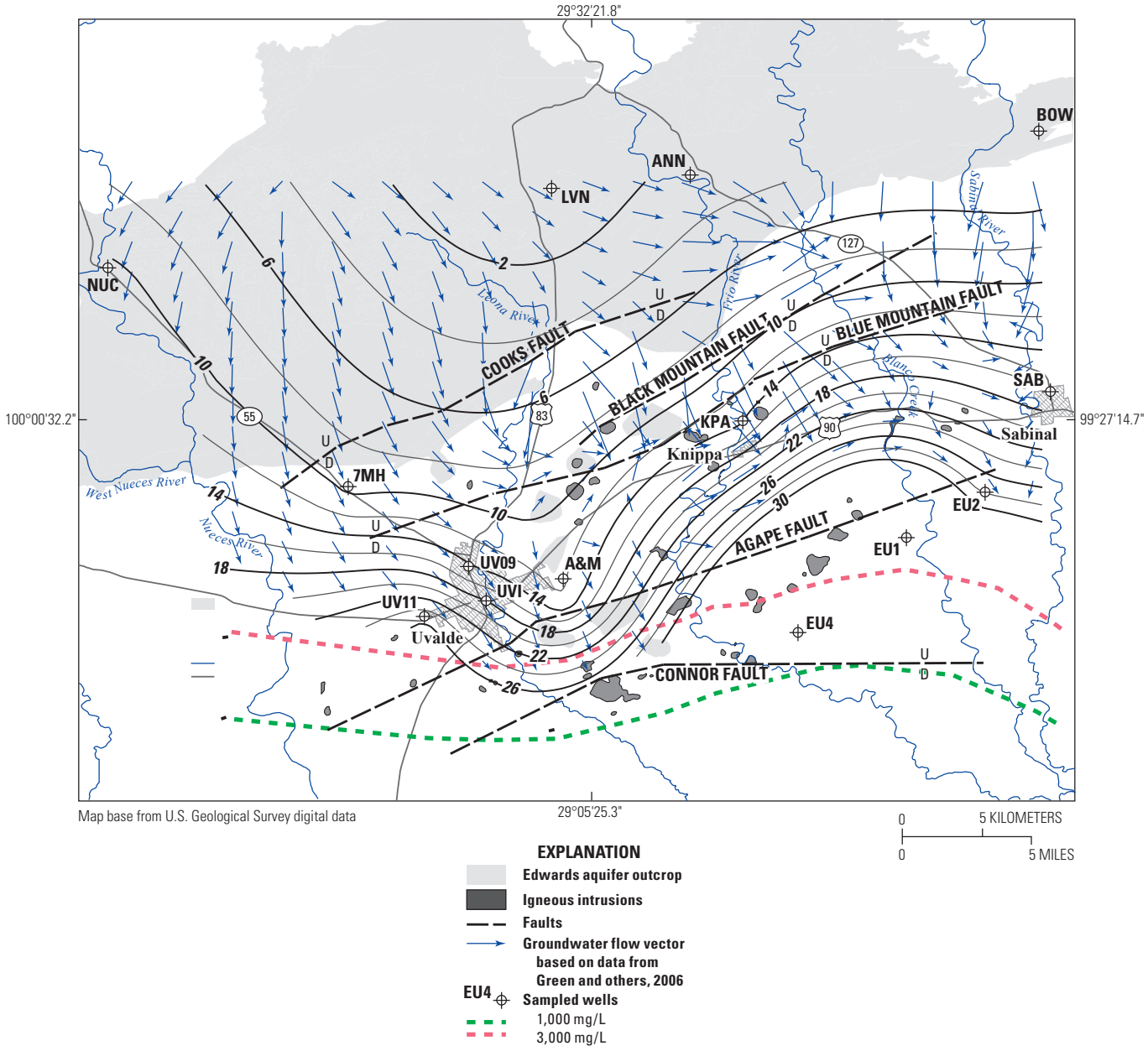

Figure 6. Contour of apparent age (^{3}H-^{3}He) with flow vectors derived from the dataset of Green, Bertetti, and others (2006) from figure 2. Age contours intervals (bold and normal solid lines) are in two year intervals.

be related to enhanced hydraulic conductivity associated with an unknown structure. Flow vectors mimic this trend, flowing southward until reaching a potentiometric trough locally known as the "Knippa Gap" north of the city of Uvalde. Generally flow vectors follow the apparent age gradient; however, the presence of a groundwater high east of the city of Uvalde reverses groundwater flow direction against the apparent age gradient. The resultant vectors indicate that the groundwater is becoming younger with increasing flow path. This is not possible and probably results from a lack of data points in the groundwater trough. In terms of the regional scale flow system, the apparent age values correlate well to the groundwater flow representation as determined from the potentiometric surface.

Samples from the recharge zone of the Edwards aquifer show a consistent older age component (about 4 to 10 years) where samples are expected to be extremely young, that is associated with streambed infiltration. As noted previously, the ANN recharge temperature was cooler than expected for the area. The anomalous temperature was attributed to rapid infiltration associated with the nearby Frio River. The age would be expected to be less than 0.5 years (no resolvable ^{3}He*) but instead the data for the sample give an apparent age of 3.2 years. Similar older ages are observed in NUC and BOW samples that share close proximity to the Nueces and Sabinal Rivers. This age anomaly could be explained by localized, subsurface discharge of modern groundwater from the

Trinity aquifer, providing an apparent mixed age associated with the interaction between the aquifers. Another explanation is that the waters associated with streambed infiltration are a result of groundwater discharge of modern groundwater in the catchments north of the Edwards aquifer recharge zone. The discharge waters do not re-equilibrate with the atmosphere rapidly and end up recharging the Edwards aquifer with excess ^{3}He*. Both arguments are probable but cannot be fully addressed with the present dataset.

Even though the data are sparse, a mass balance model can be inferred. Groundwater flow from the northwestern part of the study area is considered to be a part of the Uvalde "pool" of the Edwards aquifer (Green, Bertetti, and others, 2006). The "pool" is characterized by recharge associated with the Nueces, Frio, and Dry Frio River Basins and discharges into the San Antonio "pool" through the Knippa Gap. Green and others (2006) predicted that the amount of water moving through the gap was on the order of 270,000 acre-feet per year (acre-ft/yr) (approximately 3.3×10^{8} m^{3}/yr). Assuming the apparent age from sample KPA (14.3 years) represents the residence time of the water in the reservoir (Uvalde "pool"), the reservoir size is estimated to be 3,861,000 acre-ft (approximately 4.7×10^{9} m^{3}). Equating this value to saturated volume in the aquifer is difficult because of the sensitivity of the calculation to effective porosity and thickness of the aquifer, but does give a scale of storage associated within the segment of the aquifer. Beyond this type of simple calculation, further data would be needed to equate the validity of flux estimates as well as other possible sources of discharge from the aquifer.

Summary

^{3}H-^{3}He ages of groundwater within the freshwater zone of the Edwards aquifer within Uvalde County show a strong modern component. The modern ages and dissolved gas compositions of the fresh groundwater reflect an active flow system, bounded by a more stagnant saline-water zone that is considerably older in age. Dissolved gas, thermal, and conductivity data support a zone of mixing occurring between the freshwater and saline-water zone, as well as mixing of premodern freshwater components of the aquifer. The nature of groundwater flow along this transition zone is complex because of structural controls and karst features of the aquifer. The older ages and presence of excess He in wells within the northern recharge zone suggest the possibility of subsurface discharge from the Trinity aquifer, and could be a factor in determining total recharge for the area. Vertical velocities from single monitoring wells support a point-sourced recharge from streambed infiltration. Overall, the trend in age distribution across the aquifer follows inferred flow patterns from the potentiometric surface and appears to support conceptual models of groundwater flow.

References Cited

Aeschbach-Hertig, W., Peeters, F., Beyerle, U., and Kipfer, R., 1999, Interpretation of dissolved atmospheric noble gases in natural waters: Water Resource Research, v. 35, p. 2779–2792.

Ballentine, C.J., Burgess, R., and Marty, B., 2002, Tracing fluid origin, transport and interaction in the crust, *in* Porcelli, D., Ballentine, C.J., and Wieler, R., eds., Noble gases in geochemistry and cosmochemistry: Reviews in mineralogy and geochemistry: Washington D.C., Mineralogical Society of America, p. 481–538.

Ballentine, C.J., and Hall, C.M., 1999, Determining paleotemperature and other variables by using an error-weighted, nonlinear inversion of noble gas concentrations in water: Geochimica et Cosmochimica Acta, no. 63, p. 2315–2336.

Bayer, R., Schlosser, P., Bonisch, G., Rupp, H., Zaucker, F., and Zimmek, G., 1989, Performance and blank components of a mass spectrometric system routine measurement of helium isotopes and tritium by ^{3}He ingrowth method, Sitzungsberichte der Heidelberger Akademie der Wissenschaften. Mathematisch-naturwissenschaftliche Klasse: Heidelberg, Springer Verlag, p. 241–279.

Beardsmore, G.R., and Cull, J.P., 2001, Crustal heat flow—A guide to measurement and modelling (1 ed.): New York, Cambridge University Press, 324 p.

Bosch, A., and Mazor, E., 1988, Natural gas association with water and oil as depicted by atmospheric noble gases—Case studies from the south eastern Mediterranean coastal plain: Earth and Planetary Science Letters, v. 87, p. 338–346.

Clark, A.K., and Journey, C.A., 2006, Flow paths in the Edwards Aquifer, northern Medina and northeastern Uvalde Counties, Texas, based on hydrologic identification and geochemical characterization and simulation: U.S. Geological Survey Water-Resource Investigation Report 2006–5200, p. 48.

Clark, A.K., 2003, Geologic framework and hydrogeologic characteristics of the Edwards Aquifer, Uvalde County, Texas: U.S. Geological Survey Water-Resource Investigation Report 2003–4010, p. 17.

Clark, A.K., and Small, T.A., 1997, Geologic framework of the Edwards Aquifer and upper confining unit, and hydrogeologic characteristics of the Edwards Aquifer, south-central Uvalde County, Texas: U.S. Geological Survey Water-Resource Investigations Report 1997–4094, p. 11.

Clark, I., and Fritz, P., 1999, Environmental isotopes in hydrology: New York, Lewis Publishers.

Clark, W.B., Jenkins, W.J., and Top, Z., 1976, Determination of tritium by mass spectrometric measurements: International Journal of Applied Radioactive Isotopes, v. 27, p. 515–522.

Ewing, T.E., and Barker, D.S., 1986, Late Cretaceous igneous rocks of the Uvalde area, southwest Texas: San Antonio, South Texas Geological Society Guidebook, p. 1–5.

Ewing, T.E., and Caran, S.C., 1982, Late Cretaceous volcanism in south and central Texas—Stratigraphic, structural and seismic models: Gulf Coast Association of Geological Societies, v. 32, p. 137–145.

Green, R.T., Bertetti, F.P., Franklin, N.M., Morris, A.P., Ferrill, D.A., and Klar, R.V., 2006, Evaluation of the Edwards Aquifer in Kenney and Uvalde Counties, Texas. Technical report prepared for the Edwards Aquifer Authority, available online at: http://www.edwardsaquifer.org/documents/2006_Green-etal_KinneyUvaldeEvaluation.pdf, 113 p.

Heaton, T.H.E., and Vogel, J.C., 1981, "Excess air" in Groundwater: Journal of Hydrology, v. 50, p. 201–216.

International Atomic Energy Agency, 2004, Isotope hydrology information system: Isotope Hydrology Information System database, available at http://isohis.iaea.org.

King, W., and Simmons, G., 1972, Heat flow near Orlando, Florida and Uvalde, Texas determined from well cuttings: Geothermics, v. 1, no. 4, p. 133–139.

Kipfer, R., Aeschbach-Hertig, W., Peeters, F., and Stute, M., 2002, Noble gases in lakes and ground waters, *in* Porcelli, D., and Ballentine, C.J., eds., Noble gases in geochemistry and cosmochemistry: Reviews in Mineralogy and Geochemistry, volume 47, p. 615–690.

Lucas, L.L., and Unterweger, M.P., 2000, Comprehensive review and critical evaluation of the half-life of tritium: Journal of Research of the National Institute of Standards and Technology, v. 105, p 541–549.

Marine, I.W., 1979, The use of naturally occurring helium to estimate groundwater velocities for studies of geologic storage of radioactive waste: Water Resources Research, v. 15, no. 5, p. 1130–1136.

Mazor, E., 1993, Interrelations between groundwater dating, paleoclimate and paleohydrology. In: Applications of Isotope Techniques in the Study of the Past and Current Environmental Changes in the Hydrosphere and the Atmosphere, International Atomic Energy Agency, Vienna, p. 249–257.

Mazor, E. and Bosch, A., 1992 Helium as a semi-quantitative tool for groundwater dating in the range of 104 to 108 years: Isotopes of Noble Gases as Tracers in Environmental Studies, International Atomic Energy Agency, Vienna, p. 163–178.

Miggins, D.P., Blome, C.D., and Smith, D.V., 2004, Preliminary $^{40}Ar/^{39}Ar$ geochronology of igneous intrusions from Uvalde County, Texas—Defining a more precise eruption history for the southern Balcones Volcanic Province: U.S. Geological Survey Open-File Report 2004–1031, p. 14.

National Oceanic and Atmospheric Administration, 2006, General local climate information, Uvalde TX: http://www.srh.noaa.gov/ewx/.

Schlosser, P., 1992, Tritium/ (super 3) He dating of waters in natural systems, *in* Loosli, H.H., and Mazor, E., eds., Isotopes of noble gases as tracers in environmental studies: Panel Proceedings Series, International Atomic Energy Agency: Vienna, Austria, International Atomic Energy Agency, p. 123–145.

Shultz, A.L., 1994, Review and update of the position of the Edwards aquifer freshwater/saline-water interface from Uvalde to Kyle, Texas: Edwards Underground Water District Report 94–05, p. 31.

Smith, D.V., Smith, B.D., and Hill, P.L., 2002, Aeromagnetic survey of Medina and Uvalde Counties, Texas: U.S. Geological Survey Open File Report 2002–49.

Solomon, D.K., and Cook, P.G., 2000, ^{3}H and ^{3}He, *in* Cook, P.G., and Herczeg, A.L., eds., Environmental tracers in subsurface hydrology: Boston/Dordrecht/London, Kluwer Academic Publishers, p. 397–424.

Solomon, D.K., Hunt, A., and Poreda, R.J., 1996, Source of radiogenic helium 4 in shallow aquifers—Implications for dating young groundwater: Water Resources Research, v. 32, no. 6, p. 1805–1813.

Solomon, D.K., Poreda, R.J., Cook, P.G., and Hunt, A., 1995, Site characterization using $^{3}H/^{3}He$ ground-water ages, Cape Cod, MA: Ground Water, v. 33, no. 6, p. 988–996.

Stute, M., and Sonntag, C., 1992, Palaeotemperatures derived from noble gases dissolved in groundwater and in relation to soil temperature, *in* Loosli, H.H., and Mazor, E., eds., Isotopes of noble gases as tracers in environmental studies: Panel Proceedings Series, International Atomic Energy Agency: Vienna, Austria, International Atomic Energy Agency, p. 111–122.

Torgersen, T., and Clarke, W.B., 1985, Helium accumulation in groundwater I: and evaluation of sources and the continental flux of ^{4}He in the Great Artesian Basin, Australia: Geochimica et Cosmochimica Acta, v. 49, p. 1211–1218.

Torgersen, T., and Ivey, G.N., 1985, Helium accumulation in groundwater II—A model for the accumulation of the crustal ^{4}He degassing flux: Geochimica et Cosmochimica Acta, v. 49, no. 11, p. 2445–2452.

U.S. Census Bureau, 2008, Annual estimates of the population for counties of Texas: available online at http://www.census.gov/popest/counties/tables/CO-EST2007-01-48.xls.

Vogel, J.C., 1967, Investigation of groundwater flow with radiocarbon, in Isotopes in hydrology: In: Symposium on isotopes in hydrology; International Atomic Energy Agency, Vienna, p. 355–369.

Woodruff, C.M., and Foley, D., 1985, Thermal regimes of the Balcones/Ouachita Trend, central Texas: Gulf Coast Association of Geological Societies, v. 35, p. 287–292.

Appendix

Geophysical logs from East Uvalde 2 well from November 2002 and November 2005, Uvalde Index well, Seven Mile Hill well, East Uvalde 1 well, and East Uvalde 4 well. Bottom of well casing (BOC) and water level depths are given in feet below ground surface. Logging parameters of temperature and specific conductance are in units of degrees Celsius (°C) and millisiemens per meter (mS/m), respectively.

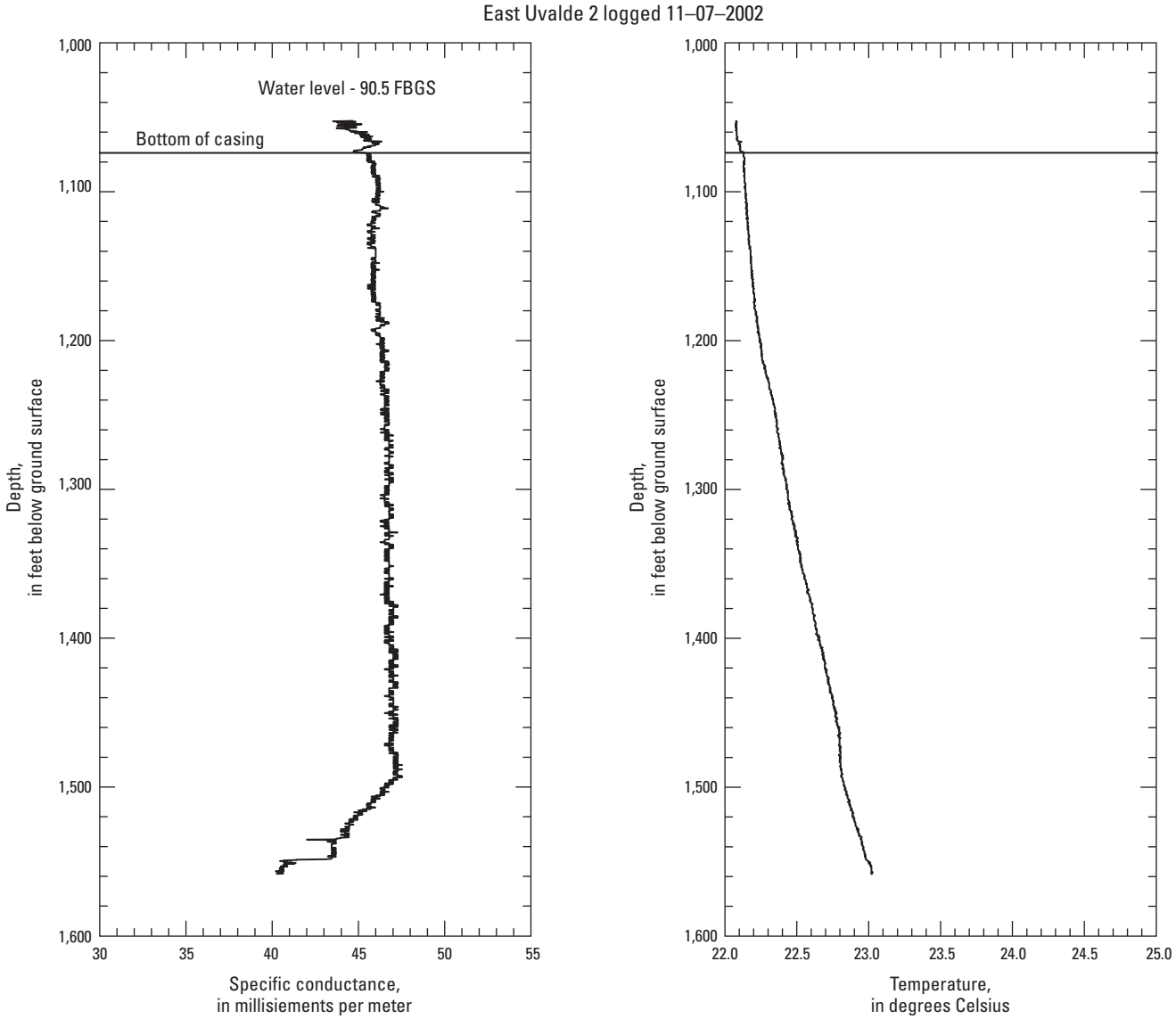

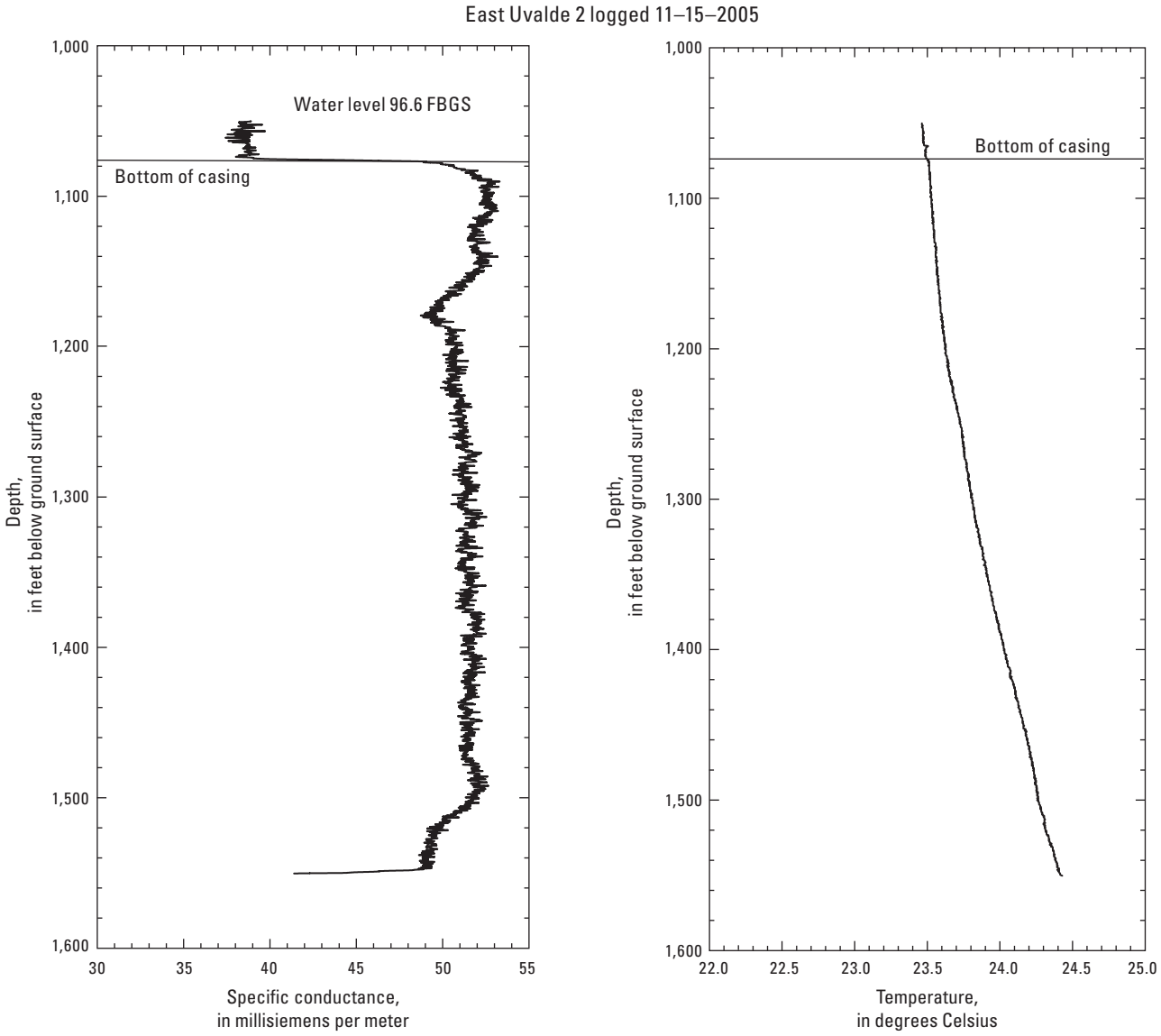
East Uvalde 2 logged 11–15–2005
Water level 96.6 FBGS
Bottom of casing
Depth, in feet below ground surface
1,000
1,100
1,200
1,300
1,400
1,500
1,600
30
35
40
45
50
55
Specific conductance, in millisiemens per meter
Bottom of casing
22.0
22.5
23.0
23.5
24.0
24.5
25.0
Temperature, in degrees Celsius

Uvalde Index Well logged 11–16–2005

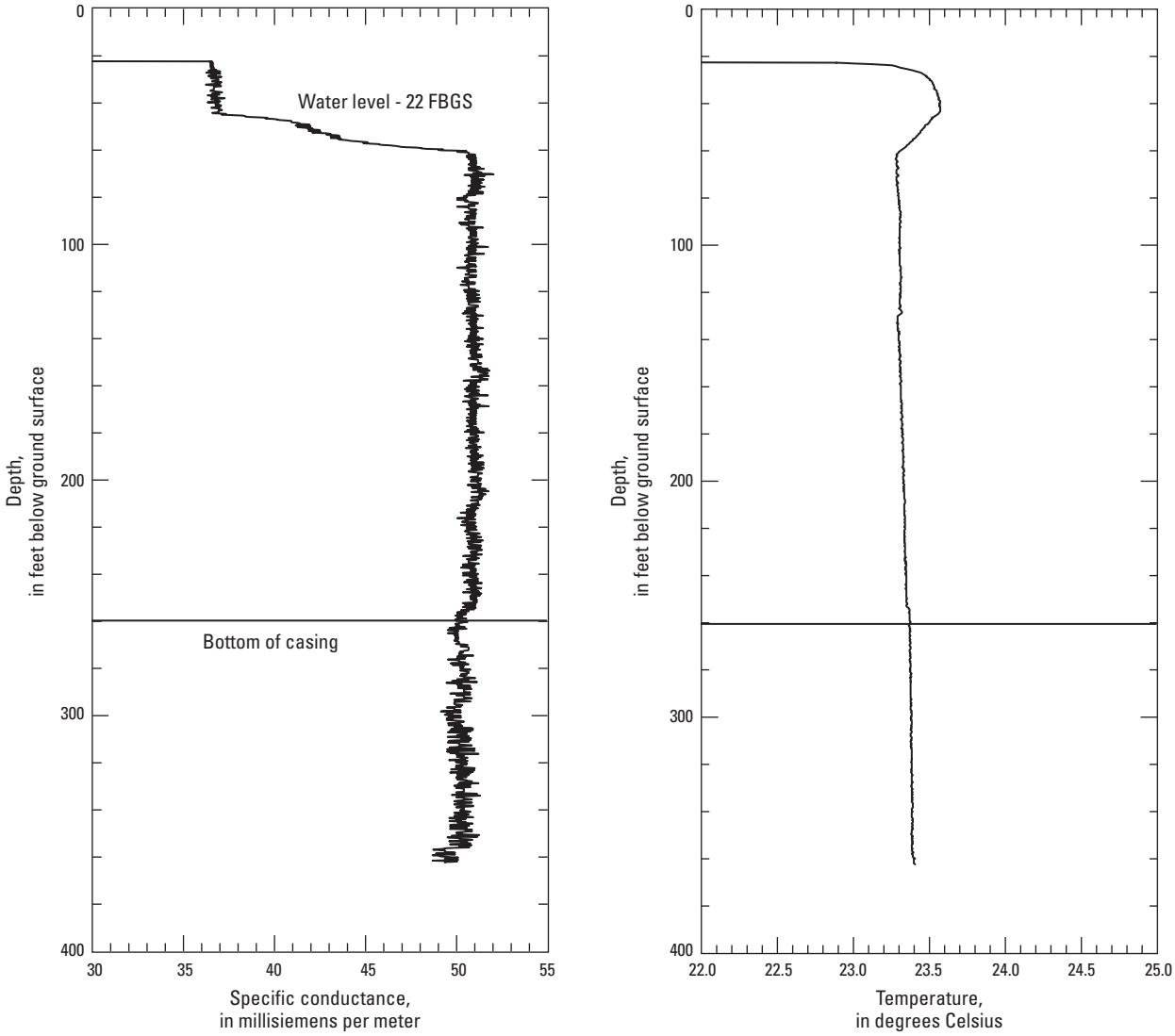

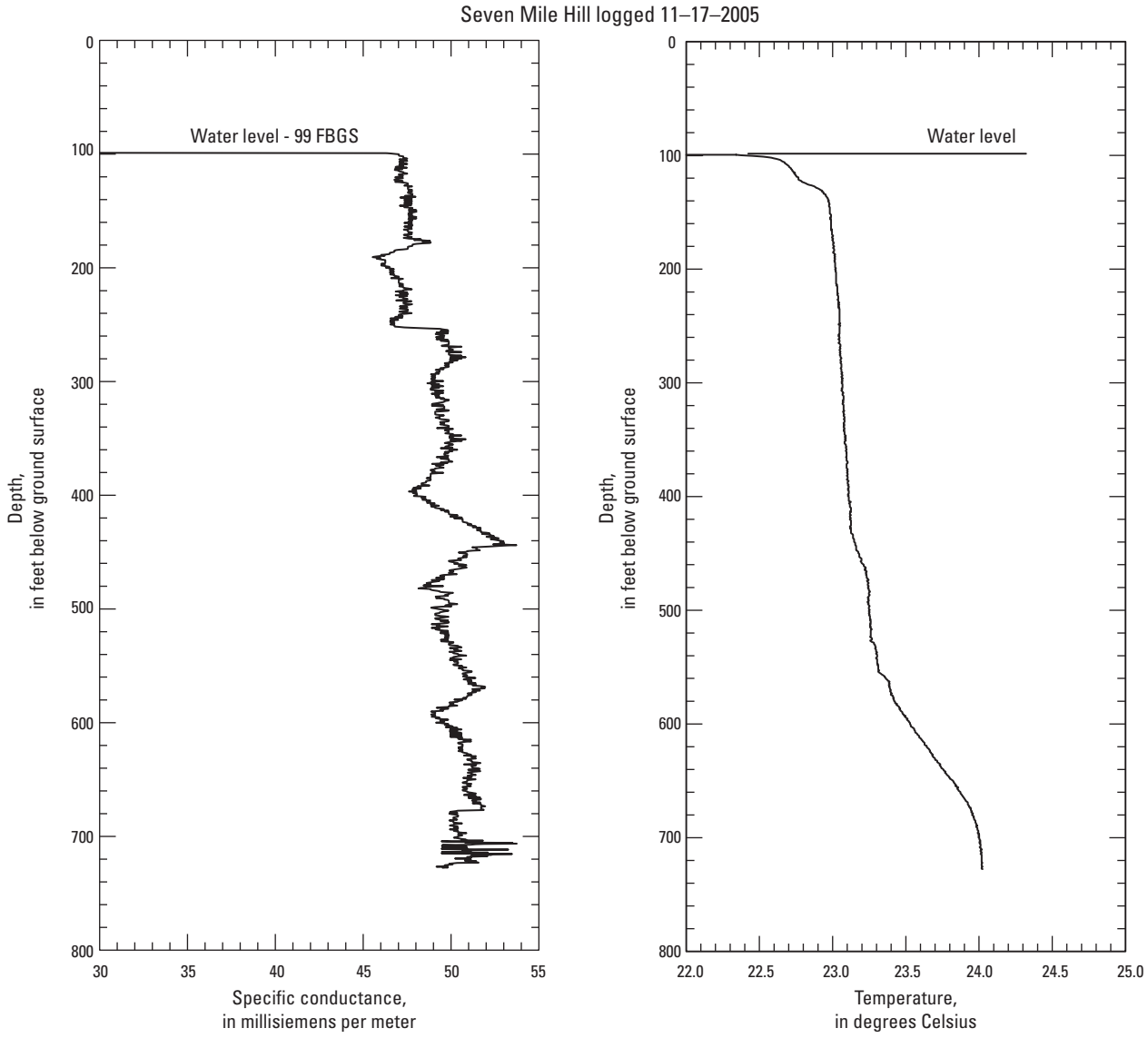
Seven Mile Hill logged 11–17–2005
Water level - 99 FBGS
Depth, in feet below ground surface
Specific conductance, in millisiemens per meter
Water level
Temperature, in degrees Celsius

East Uvalde 1 logged 11-07-2002

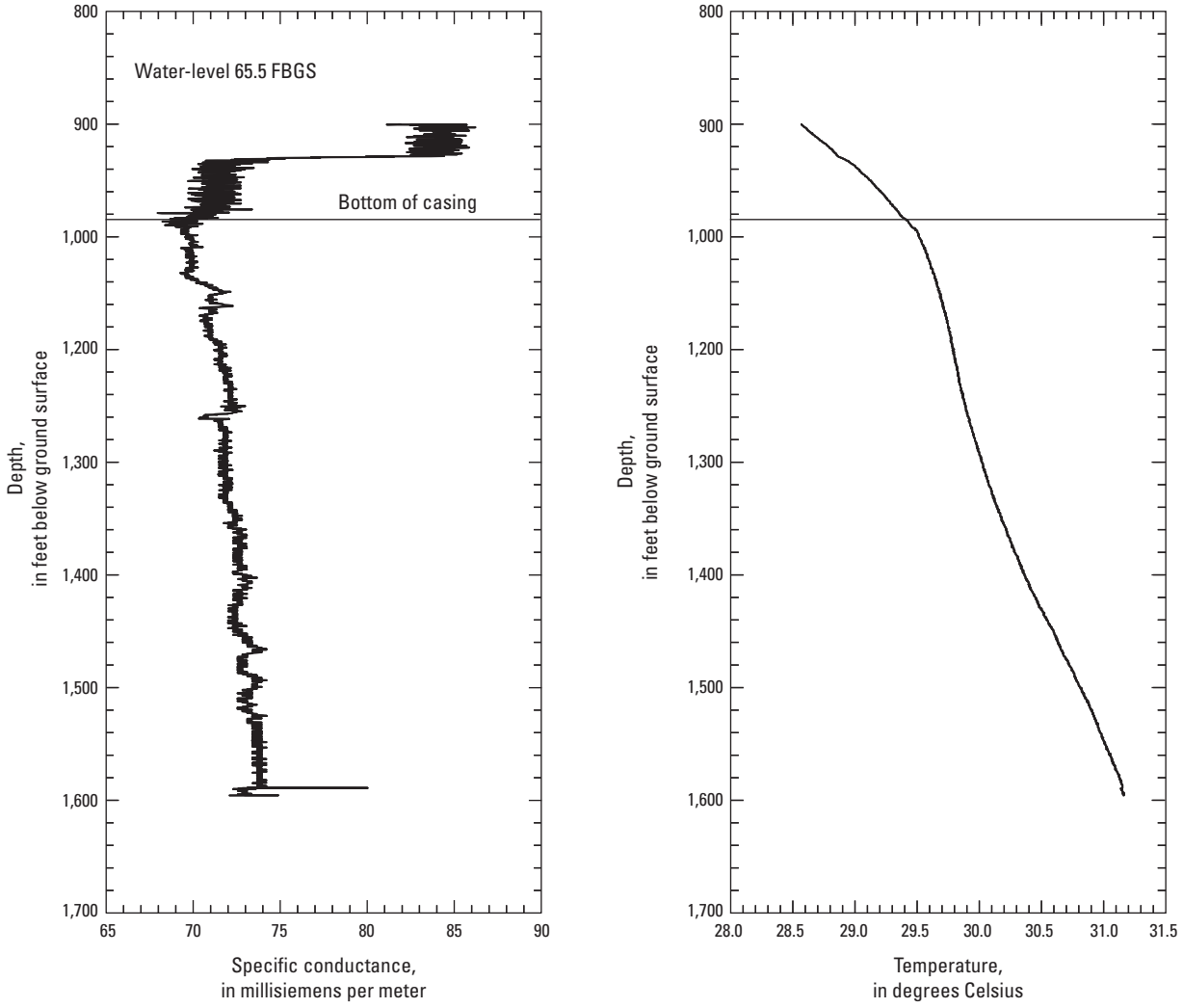

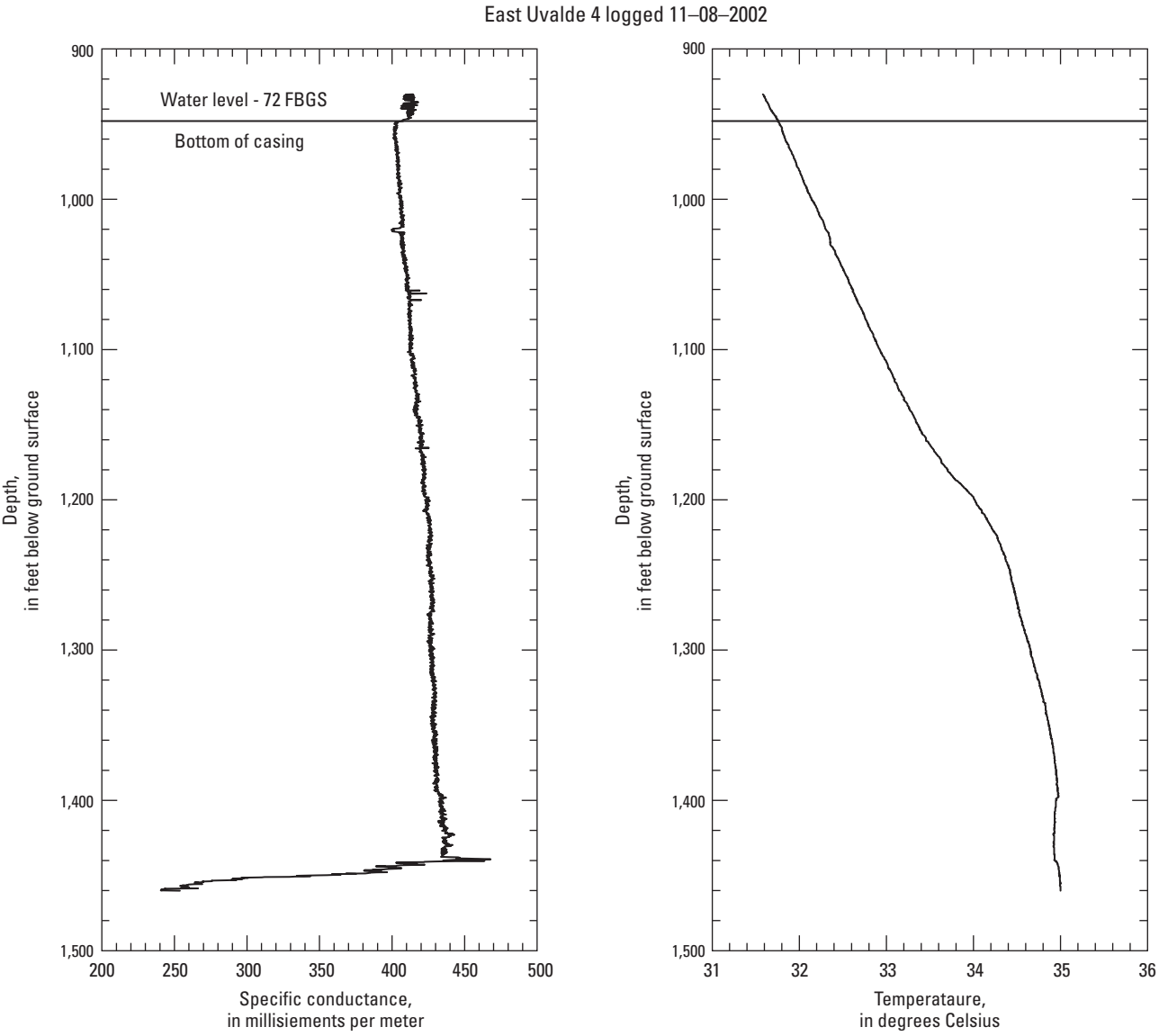
East Uvalde 4 logged 11–08–2002
Water level - 72 FBGS
Bottom of casing
Depth, in feet below ground surface
900
1,000
1,100
1,200
1,300
1,400
1,500
200
250
300
350
400
450
500
Specific conductance, in millisiements per meter
31
32
33
34
35
36
Temperataure, in degrees Celsius

Publishing support provided by:
Denver Publishing Service Center, Denver, Colorado

For more information concerning this publication, contact:

Center Director, USGS Crustal Geophysics and Geochemistry Science Center
Box 25046, Mail Stop 964
Denver, CO 80225
(303) 236-1312

Or visit the Crustal Geophysics and Geochemistry Science Center Web site at:

http://crustal.usgs.gov/

This publication is available online at:
http://dx.doi.org/10.3133/sir20155163

ISSN 2328-0328 (online)
http://dx.doi.org/10.3133/sir20155163